UNIVERSITY OF GHANA, LEGON

COLLEGE OF BASIC AND APPLIED SCIENCES

UNDERSTANDING THE INFLUENCE OF THE DYNAMICS OF MOISTURE CONVERGENCE ON RAINFALL IN WEST AFRICA

By

Ebenezer Nyarko Jessey Biney

(10803812)

A THESIS SUBMITTED TO THE SCHOOL OF GRADUATE STUDIES IN PARTIAL FULFILMENT OF THE REQUIREMENT FOR THE AWARD OF THE DEGREE OF MASTER OF PHILOSOPHY IN PHYSICS

DEPARTMENT OF PHYSICS

July 2022.

DECLARATION

I hereby declare that this submission is my own work and that, to the best of my knowledge, it contains no material previously published by another person nor materials which have been accepted for the award of any other degree of the university, except where due acknowledgment has been made in the text.

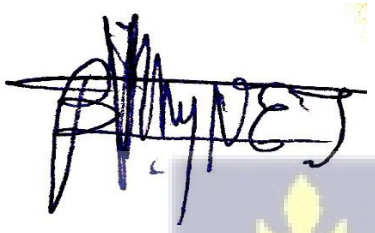

..... Date: 10-10-2023

EBENEZER NYARKO JESSEY BINEY
(Candidate: 10803812)

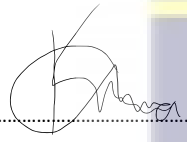

..... Date: 23/10/2023

PROF. NANA AMA BROWNE KLUTSE
(Supervisor)

DEDICATION

This thesis is dedicated to my beautiful family.

ACKNOWLEDGMENT

I am sincerely grateful to everyone who contributed by any means to make this work successful. I feel obliged to acknowledge the following persons for their special contribution to the completion of this study.

First, I am deeply grateful to my supervisors Prof. Nana Ama Browne Klutse and Dr. Hubert Azoda Koffi for our useful discussions throughout my study. I thank Emeritus Prof. J.K.A. Amuzu, Dr. V.C.K. Kakane, Dr. M.N.Y.H. Egblewogbe, Dr. Felix Allison Hughes, Dr. Ato Yankson, Dr. G.K. Nkrumah-Buandaoh, Dr. Godfred Bright Hagan, and Dr. Samuel A. Atarah who are all lecturers in the Department of Physics, University of Ghana for their support and encouragement. I am also grateful to my good friend Gideon Darko, Francis Adea Michael Anakwah, and Addo Sowah, my colleague M.Phil. Candidates in the Department of Physics.

Finally, my heartfelt gratitude to all my family members for their support throughout my study period.

ABSTRACT

The main goal of this study is to thoroughly examine the behavior of vertically integrated moisture flux convergence (MFC) and moisture flux across West Africa. We aim to gain valuable insights into how these complex atmospheric processes relate to rainfall patterns. The study covers two significant time spans: 1981 to 2005, allowing us to analyze historical trends, and 2006 to 2100, providing a look ahead in the context of potential climate shifts. To conduct this study, we have heavily relied on robust datasets. The Climate Research Unit observational datasets and ERA-5 data from 1981 to 2005 have formed a strong foundation for our analysis. Additionally, we have used model outputs from the Coordinated Regional Down-scaling Experiment (CORDEX)-Africa to enhance the comprehensiveness of our research and accurately depict climatic conditions. To calculate moisture flux convergence (MFC), we carefully processed specific humidity, rainfall, and evaporation data extracted from the selected datasets. Similarly, we integrated specific humidity and horizontal wind data to compute moisture flux. These calculations, forming the core of our study, have revealed a noticeable difference in impact between MFC and wind convergence. Specifically, we computed characteristic impact values of 2.53mm/day and 1.6mm/day for MFC and wind convergence, respectively. One of the key findings of this research highlights the predominant influence of MFC on precipitation. This is supported by a strong positive correlation of 0.8315 observed between MFC and rainfall across the expansive West African region (WA), emphasizing the significant role of considering moisture flux dynamics in understanding and predicting rainfall patterns. Furthermore, our analysis involved computing the Rainfall Anomaly Index. This computation provided valuable insights into the changing pattern of drought occurrences. Notably, we observed a decline in drought incidence during the mid-21st century, followed by an increase towards the end of the century. This cyclic pattern suggests an increased likelihood of the region experiencing drier conditions as we progress further into the century.

TABLE OF CONTENTS

LIST O F TABLES

LIST OF FIGURES

LIST OF ACRONYMS

CHIRPS……..…Climate Hazards Group InfraRed Precipitation with Station Data

CORDEX……..…Coordinated Regional Downscaling Experiment.

CRU….. ……..…Climatic Research Unit

ECMWF...…....…European Centre for Medium-Range Weather Forecast

GFS……...Global Forecast System

ITD……...…....…Intertropical discontinuity

IVT……...…Integrated Water Vapor Transport

JJAS ….....……...June July August September

MAM…..…….… March April May

MBE……...… Mean Bias Error

MFC……....Moisture Flux Convergence

MFCAI……Moisture Flux Convergence Anomaly Index

NCEP……...National Centers for Environmental Prediction

NCAR……...…...National Center for Atmospheric Research

NDJF……November December January February

RAI……...The Rainfall Anomaly Index

RCP……....Representative Concentration Pathway

RMSE……...Root Mean Square Error

VIMD……...Vertically Integrated Moisture Divergence

VIMC…….....Vertically Integrated Moisture Convergence

WA……..West Africa

WAM……..West Africa Monsoon

CHAPTER 1

INTRODUCTION

This chapter captures the background of the study, the research problem and justification, the objectives of the study, and the organization of the study.

1.1 Background

West Africa is a region characterized by a diverse climate and an agrarian economy heavily dependent on seasonal rainfall. Adequate and reliable rainfall is vital for agricultural productivity and sustenance of the region's ecosystem. The drought that afflicted West African nations in the early 1970s lasted for years and is regarded as "one of the most undeniable and significant contemporary climatic shifts identified by the climate scientific community" (Aiguo et al., 2004). This resulted in famines that struck West Africa in the 1970s (1972–74) and the 1980s (1983–85), prompting several authors (e.g., Folland et al. 1986; Hastenrath 1990; Lamb and Peppler 1992; Fontaine and Janicot 1996) to investigate potential mechanisms underlying these dramatic events (Le Barbé et al., 2002).

The climate in West Africa is strongly influenced by the West African Monsoon (WAM), a major component of the global monsoon system. The West African Monsoon (WAM) is a prominent atmospheric circulation pattern that brings about the seasonal shift in winds, leading to wet and dry seasons. The monsoon season is a critical determinant of agricultural success, food security, and overall socioeconomic well-being for millions of people in this region.

This monsoon manifests as a seasonal reversal of wind patterns and is characterized by distinct wet and dry phases. During boreal summer (June to September), warm, moist air from the Gulf of

Guinea and the Atlantic Ocean is drawn northwards due to low-level atmospheric pressure over the continent, resulting in a southwesterly airflow. This moist air converges with dry continental air from the Sahara Desert, culminating in the formation of the Intertropical Convergence Zone (ITCZ). The ITCZ is a region of intense convective activity and rainfall, essential for the sustenance of vegetation, agriculture, and ecosystems across West Africa.

Conversely, during boreal winter (November to March), the atmospheric pressure reverses due to the southward migration of the Sun, causing a shift in wind patterns. Dry, harmattan winds prevail, originating from the Sahara and Sahel regions, leading to reduced humidity and clear skies. This marks the dry season, with minimal rainfall and higher temperatures across much of West Africa.

The West African Monsoon is a complex interplay of various atmospheric and oceanic factors. Key components include the African Easterly Jet (AEJ), African Easterly Waves (AEWs), and the Saharan Air Layer (SAL). The AEJ, for instance, influences the African easterly flow, while AEWs, originating from the Sahel, contribute to disturbances in the monsoon circulation. Additionally, the SAL, comprising dry and dusty air from the Sahara, can impact cloud formation and suppress convection during the monsoon season.

Advancements in meteorological and climatological research, as well as the availability of high-resolution climate models and improved satellite technologies, offer an opportunity to delve deeper into these dynamics. Many specialized indicators based on available data, such as precipitation, specific humidity, evapotranspiration, Zonal and Meridional winds, and temperature, have been established to monitor droughts and wet periods and investigate their variability. (Heim 2000; Keyantash and Dracup 2002; Wang et al., 2015). Among these indices is the Rainfall anomaly index.

It is of great importance to study the factors that directly influence rainfall for effective predictions. The relative contribution of various moisture sources to precipitation in a region may be determined using quantitative moisture transport analysis. The study focuses on moisture flux convergence (MFC), the Rainfall anomaly index (RAI), and the MFC anomaly index to study the historical trend in rainfall and its projection to the end of the twenty-first century.

This research endeavor seeks to make a valuable contribution to the broader comprehension of climate variability in West Africa through the comprehensive examination of the intricate mechanisms governing the convergence of moisture flux and its profound influence on the intricate patterns of rainfall. It is believed that moisture flux convergence (MFC) directly describes the behavior of intense rainfall occurrences (Chou et al.2009 and Zhou et al.2017).

1.2 Research Problem and Justification

The role and extent of related mechanisms such as aerosol fluctuations, Sea surface temperature, vegetation, and soil and atmospheric moisture in the recovery from drought in West Africa during the 1960s and 70s is still not fully understood (Okoro et al., 2020).

Accurate weather and climate forecasting of rainfall is critical for anticipating catastrophic events (such as floods and droughts) and making sure there is food and water security in the face of climate change. They are especially important in West Africa, where populations are more vulnerable to climate change than anywhere else. Significant progress has been achieved in the last ten years, but much work remains to be done to accurately forecast heavy rains and droughts (Gimeno, Dominguez, Nieto, Trigo, Drumond, Reason, Taschetto, Ramos, & Kumar, 2016).

Moisture fluxes from a variety of sources, such as soil moisture and the atmospheric moisture flux convergence, result in WAM precipitation (Dyn et al., 2016). Understanding the nature of these

moisture fluxes is critical to comprehending WAM variability. It is in this light that this study is conducted to throw more light on the influence of the dynamics of moisture flux convergence on rainfall in West Africa.

1.3 Aim of the study

To determine how the dynamics of moisture flux convergence influence rainfall in West Africa.

1.4 Specific Objectives

The specific objectives of the study are as follows:

1. to analyze how moisture flux influences rainfall in West Africa.
2. to analyze how moisture flux influences rainfall in West Africa.
3. to utilize CORDEX models (RCA4 and RACMO22T) to assess rainfall variability in West Africa from 2006 to 2100.

1.5 Significance of the Study

This research leverages two CORDEX datasets and the ERA-5 dataset to compute Moisture Flux, Moisture Flux Convergence, Rainfall Anomaly Index, and Moisture Flux Convergence Anomaly Index to understand their relationship with rainfall patterns in West Africa. These computed indices are then used to analyze rainfall variability in West Africa throughout the twenty-first century.

1.6 Organization of the Dissertation

There are five chapters in the dissertation. The first chapter discusses the study's background, which includes an introduction, problem statement, objectives, significance of the study, and scope of the study. The second chapter is a review of related literature and is based on other research

findings related to this study. The study area, data used, error analysis on the data used as well as calculation of MFC and other statistical analyses are captured in chapter three. Chapter four contains the results and discussion of this study. Conclusions and Recommendations are included in Chapter 5.

CHAPTER 2

LITERATURE REVIEW

The mathematical formulas and statistical instruments used in the study are presented in this chapter. The research region is described first, and then the physical expression of moisture flow and moisture flux convergence is derived. This chapter presents fundamental statistical analysis using graphical tools and fundamental statistics such as mean bias error, absolute error, root mean square error, anomaly index, and regression analysis. This chapter also covers the datasets that were utilized in the study.

The West African Monsoon (WAM), occurring from June to September, and the East African Monsoon, which prevails from March to May, play crucial roles in shaping the rainfall patterns over West Africa. The WAM is characterized by the prevailing southwesterly winds from the Atlantic Ocean during the warmer months, carrying moisture into the land (Sylla et al., 2013). This monsoon system accounts for approximately 70% of the yearly precipitation in the region and is significantly influenced by geographic features such as the Guinea highlands, the Jos Plateau, and the Cameroon Mountains (Klutse et al., 2021).

The atmospheric moisture flow of the West African monsoon (WAM) significantly influences the amount of rain produced by synoptic-scale systems (Cook, 2018). Rainfall during the WAM season is a result of moisture fluxes from various sources, including soil moisture and the convergence of atmospheric moisture fluxes (Sultan & Janicot, 2003; Mera et al., 2014; Lélé et al., 2015; Kumar et al., 2016). Understanding these moisture sources is vital to comprehend the variability of rainfall in West Africa.

One of the most critical challenges faced by sub-Saharan West African nations is the fluctuation in water availability, limiting their capacity to sustain life, agriculture, and economic growth. In understanding WAM dynamics and variability, the involvement of atmospheric moisture transfer and related phase transitions through processes like evaporation, latent heat release, and associated energy transports and exchanges is crucial. This is because the scales of the primary circulation patterns are determined by hydrological processes (Ndehedehe et al., 2019). Yet, only a few studies have utilized observations and modeling to investigate the origins of moisture transport in West Africa.

Cadet & Nnoli (1987) investigated water vapor flow across Africa and the Atlantic Ocean, with a focus on West Africa (WA) during the summer of 1979. Their study centered on vapor transport utilizing mean fields of pressure waves and their fluctuations in rainfall, as well as the level III-b wind fields from the European Centre for Medium-Range Weather Forecasts (ECMWF). The progression of moisture penetration across West Africa during the summer months can be observed in the evolution of the biweekly fields of vertically integrated mean fluxes of water vapor between 850 mb and the surface. The amount of moisture carried by the northeast trade winds around the equator also increases. A significant belt of westerlies is observed across West Africa during the complete development of the monsoon when the southerly flux reaches up to 20°N. The mostly zonal flows for the 700–500 mb layer underscore the significance of the African easterly jet as a key conduit across West Africa.

Gong & Eltahir (1996) investigated the sources of moisture for rainfall in West Africa and provided quantitative estimations of the moisture contributions from both local and external fluxes. Local evaporation as well as evaporation in the areas to the east and south of the region are the primary contributors to precipitation in West Africa. These three factors collectively account for

nearly 70% of all precipitation in West Africa. The combined evaporation from the two African landmasses contributes 44% more rain to West Africa than the tropical Atlantic Ocean does (23%). Intriguingly, local evaporation is a larger contributor to rainfall in West Africa compared to the tropical Atlantic Ocean.

Long (2000) examined the links between interannual variation in precipitation time series and general circulation characteristics such as vertical motion and vapor flux. The study demonstrated variations in behavior between the periods of June to July (JJ) and August to September (AS), as well as between the dynamics of the north and south sub-Sahara. The linear correlation coefficients for rainfall and moisture flow time series revealed these variations.

To provide a more comprehensive understanding of the mechanisms at work, Bielli et al. (2010) explored the use of NCEP/GFS operational analysis to separate the geographic scales in evaporation, precipitation, and moisture flow divergence fields. Their focus was on the two months characterized by active monsoon conditions. It's important to note that the outcomes of the investigation within this limited time frame should be considered indicative of the monsoon seasons. Bielli (2010) discovered a significant positive association between precipitation and moisture convergence, particularly on a broad scale. This association was observed both across land and the Gulf of Guinea. Although moisture convergence in the African easterly jet (AEJ) layer was strongly correlated with precipitation over the Sahel band at all scales, no strong correlation between moisture divergence and this region was found.

Lélé et al. (2015) utilized NCEP-NCAR reanalysis data to produce vertically integrated moisture flow (VIMF). Their research focused on understanding the factors influencing the surface-850 hPa transportation of moisture and moisture convergence into West Africa during the monsoon season, and how these factors affect rainfall variability. The fundamental goal was to comprehend the

interaction between large-scale atmospheric circulation, associated convergence, and precipitation events. Observations revealed significant interannual variability in moisture transport on an annual and seasonal time scale. The correlations between the components constituting moisture transport and rainfall emphasized the strong association between zonal moisture transport and Sahelian precipitation. The study identified two latitudinal locations of moisture convergence: a substantial convergence zone extending from the Sahel to Guinea's coast, peaking in the spring. This suggests that the air column in West Africa is moistened more frequently in the spring than during the busier summer months. Additionally, the research highlighted that water vapor convergence often occurs north of the equator, with the center of the largest flux convergence being south of the latitude of the intertropical front (ITF). However, further research is needed to explore the dynamics and factors influencing moisture transport comprehensively, particularly the variations in moisture convergence and divergence over different latitudinal bands.

2.1 Theoretical framework

2.1.1 Physical Expression of Moisture Flux Convergence

Using the conservation of water vapor in the pressure coordinate (p), we can derive the formula for Moisture Flux Convergence (MFC):

$$\frac{dq}{dt} = W \qquad (1)$$

Here, the expression $\frac{d}{dt} = \frac{\partial}{\partial t} + u\frac{\partial}{\partial x} + v\frac{\partial}{\partial y} + \omega\frac{\partial}{\partial p}$

u, v, and ω represent the standard three-dimensional components of the wind vector in pressure coordinates, and the letter q represents specific humidity. W stands for the amount of water vapor stored, which can be calculated as the difference between the water vapor sources and sinks due

to the movement of air parcels. In this expression, W is usually expressed as E – C, where C represents the condensation rate, and E represents the evaporation rate. Studies that employ equation (1) often do so under the assumption that the total water vapor that condenses precipitates out immediately.

Hence, W = E – P (Palmén, 1962).

Furthermore, $\frac{\partial u}{\partial x}+\frac{\partial v}{\partial y}+\frac{\partial \omega}{\partial p}=0$, which is the mass continuity equation, allows equation (1) to be re-written in flux form by expanding and adding zero to both sides of (1) (Banacos & Schultz, 2005):

$$\frac{\partial q}{\partial t}+u\frac{\partial q}{\partial x}+v\frac{\partial q}{\partial y}+\omega\frac{\partial q}{\partial p}+q\left(\frac{\partial u}{\partial x}+\frac{\partial v}{\partial y}+\frac{\partial \omega}{\partial p}\right)=E-P \qquad (2)$$

$$\frac{\partial q}{\partial t}+\frac{\partial}{\partial x}(qu)+\frac{\partial}{\partial y}(qv)+\frac{\partial}{\partial p}(q\omega)=E-P$$

$$\frac{\partial q}{\partial t}+\nabla.(qV)+\frac{\partial}{\partial p}(q\,\omega)=E-P \qquad (3)$$

2.1.2 Moisture Budget

The principal processes generating precipitation are identified by computing each term in the water balance equation (Chen & Tomassini, 2015).

Equation (3) can be re-written as:

$$-\frac{\partial q}{\partial t}-\nabla.(qV)-\frac{\partial}{\partial p}(q\,\omega)=P-E$$

Furthermore,

$$-\left\langle\overline{\frac{\partial q}{\partial t}}\right\rangle-\left\langle\overline{\nabla\cdot(qV)}\right\rangle-\left\langle\overline{\frac{\partial}{\partial p}(q\,\omega)}\right\rangle=\overline{P}-\overline{E} \qquad (3^*)$$

Here, P represents precipitation, q is specific humidity, and E represents evaporation. The vector $\vec{v}$ is the horizontal wind vector.

The operator $\nabla = \boldsymbol{i}\frac{\partial}{\partial x} + \boldsymbol{j}\frac{\partial}{\partial y}$ represents the horizontal divergence operator. The bars represent the average for the period and $\langle\cdot\rangle$ represents vertical integration $\int_{p_0}^{p_s}(\cdot)\,dp/g$. The first term on the left side, $-\left\langle\overline{\frac{\partial q}{\partial t}}\right\rangle$, represents the rate at which relative humidity is changing within the locality. $-\left\langle\overline{\nabla\cdot(qV)}\right\rangle$ represents horizontal moisture flux convergence (MFC).

$-\left\langle\overline{\frac{\partial}{\partial p}(q\ \omega)}\right\rangle$ represents vertically integrated MFC.

Pressure velocity ω is assumed to be zero close to the ground (at the surface) p_s and at the moisture upper boundary p_o.

2.1.3 Moisture Flux

The product of the field of values and the wind speed is referred to as the flux of that field.

For example,

$$\vec{Q} = n\overrightarrow{V_h} \qquad (1)$$

Where n is the specific humidity measured in grams per kilogram, and $\overrightarrow{V_h}$ is the horizontal wind speed measured in meters per second, $\vec{Q}$ is the moisture flow.

Equation (1) is normally integrated through the depth of the troposphere to obtain the Integrated Water Vapor Transport (IVT).

$$Integrated\ Water\ Vapor\ Transport = \int_{sfc}^{trops} q\overrightarrow{V_h}\ \mathrm{dz} = \frac{1}{\rho}\int_{sfc}^{850hPa} q\overrightarrow{V_h}\ \mathrm{dp} \qquad (2)$$

IVT has the unit kg $m^{-1}s^{-1}$.

One way to interpret IVT is that it measures the number of kilograms of water vapor that moves across 1 meter of distance in 1 second by the average wind in that layer. Since IVT contains a scalar multiplied by a vector, it is itself a vector quantity. It will have a direction and a magnitude, normally plotted in kgm^{-1} Over short time frames, $\vec{Q} = q\overrightarrow{V_h}$ can be interpreted as proportional to moisture advection.

2.1.4 Moisture Flux Convergence (MFC)

Assuming that q at the top level p_o taken at the surface p_s has zero values, $-\left\langle \overline{\frac{\partial}{\partial p}(q\ \omega)} \right\rangle$ of equation (3*) is then taken to be zero (Chou and Lan 2012). As the contribution of $-\left\langle \overline{\frac{\partial q}{\partial t}} \right\rangle$ to precipitation is very small, the term is neglected (Zhu 2007). As a result, the water balance of JJAS precipitation in West Africa is mostly determined by variations in the horizontal MFC. The vertical integral product of specific humidity and horizontal mass convergence across the troposphere determines the MFC. Horizontal Moisture Flux Convergence is frequently abbreviated as MFC (Banacos & Schultz, 2005). The term "MFC" will henceforth be used to refer to the horizontal moisture flux convergence integrated between the surface pressure (p_s) and the upper boundary pressure (p_o) at 850 hPa. To better quantify the gathering and convergence of moisture across West Africa, MFC is broken down as follows (van Zomeren & van Delden, 2007):

By vector identity, the horizontal component of MFC, $\left\langle \overline{\nabla \cdot (qV)} \right\rangle$ can be written as:

$$MFC = -\nabla \cdot (qV) = -V \cdot \nabla q - q\nabla \cdot V \qquad (4)$$

$$MFC = -u\frac{\partial q}{\partial x} - v\frac{\partial q}{\partial y} - q\left(\frac{\partial u}{\partial x} + \frac{\partial v}{\partial y}\right) \quad (5)$$

The term for advection in equation (5) denotes the horizontal advection of specific humidity, while the term for convergence denotes the product of specific humidity and the horizontal convergence of mass. Equation (3) can be solved for P - E by dividing by the acceleration of gravity, denoted by g, and then vertically integrating throughout the entire depth of the atmosphere, starting at the surface and going up to the top po (Palmén and Holopainen 1962), yielding:

$$P - E = -\frac{1}{g}\int_{p_0}^{p_s}\frac{\partial p}{\partial t}dp - \frac{1}{g}\int_{p_0}^{p_s} V \cdot \nabla q \, dp - \frac{1}{g}\int_{p_0}^{p_s} q\nabla \cdot V \, dp \quad (6)$$

Here, P stands for precipitation, and E stands for evapotranspiration from the surface, while the third term represents the MFC. ∇ is the horizontal divergence operator, and q retains its earlier definition. The MFC can be computed using the expression:

$$MFC = -\nabla\frac{1}{g}\int_{p_0}^{p_s} qVdp \quad (8)$$

The V component of the equation is written as:

$$V = u\boldsymbol{i} + v\boldsymbol{j} \quad (9)$$

Where u and v represent the components of the wind blowing in an eastward and a northward direction, respectively.

CHAPTER THREE

DATA AND METHODS

3.1 The Study Area

West Africa (or Western Africa) is the westernmost region of Africa (Figure 1). The area, which consists of 15 nations, is situated between latitudes 4° and 20°N and longitudes 17°W and 17°E. The population of West Africa is estimated at 419 million people as of 2021, with 210,967,000 males and 208,033,000 females (DESA, 2022). The area is one of the most rapidly rising regions on the African continent, both demographically and economically. There are many different ecosystems in West Africa, as well as various food production methods. The majority of the population in West Africa relies on agriculture as its primary economic engine. The three main agroecological zones in the area are the Sahel (12°–20°N), the Savanna (8°–12°N), and the Guinea Coast (4°–8°N) (Egbebiyi et al., 2019). The West African Monsoon (WAM) is responsible for approximately 70 percent of the region's annual precipitation, and it is influenced by smaller-scale highlands, including the Guinea highlands (11°N, 10°W), the Jos Plateau (10°N, 9°E), and the Cameroon Mountains (5°N, 12°E) (Quagraine et al., 2020). The WAM is a large-scale circulation characterized by a change in the direction of winds from the Atlantic Ocean that carries moisture onto the land in the lower levels of the atmosphere (Sylla et al., 2013). In West Africa, the predominant winds during the summer monsoon months (June–September) are from the southwestern part of the region, but during the dry season months (December–March), the predominant winds are from the northeast. This helps drive the seasonal rainfall pattern in the area. Additionally, the WAM monitors the location of the intertropical discontinuity (ITD) and controls the timing, variability, and distribution of precipitation across the area. This research places a

significant emphasis on the JJAS period, as it is when the area experiences the greatest amount of rainfall during the WAM months.

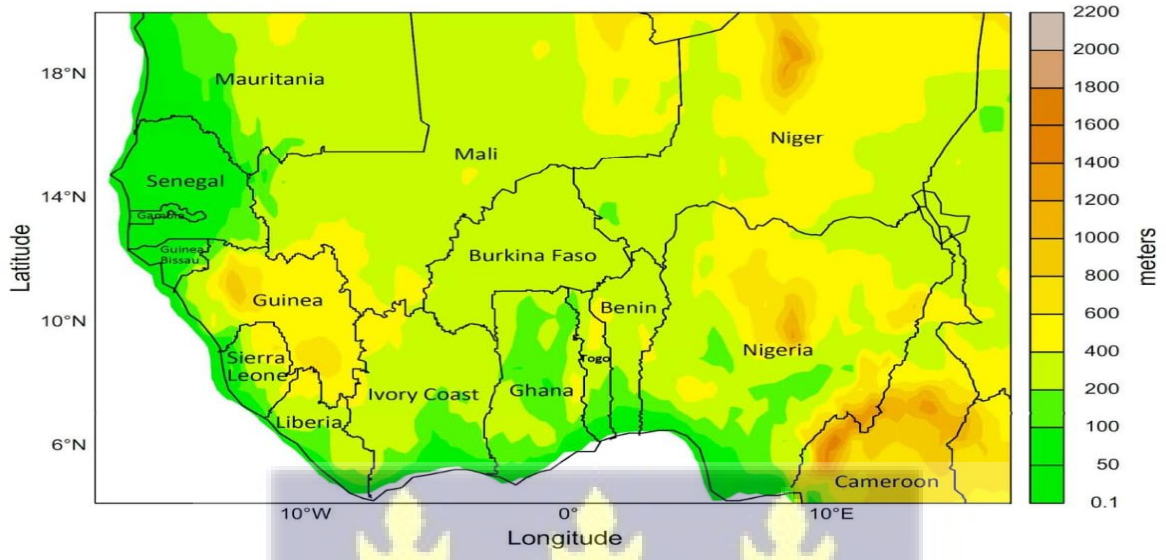

Figure 3.1: Map of West Africa with Terrain and Countries.

3.2 Methodology:

3.2.1 Moisture Flux Convergence Calculation

Mathematical methods like the divergence of moisture flux were computed using Python to calculate moisture flux convergence. This involved analyzing wind patterns and moisture content in the atmosphere, which were obtained from meteorological datasets. Python's libraries, such as NumPy for numerical computing and Pandas for data manipulation, were instrumental in processing the meteorological data efficiently.

Meteorological data containing wind patterns and moisture content were imported and organized using Pandas. Subsequently, utilizing NumPy, the mathematical calculations for divergence of moisture flux were performed based on the collected data. The calculations were implemented in a way that allowed the determination of convergence and divergence areas within the atmospheric region of interest.

Visualization of the computed convergence and divergence areas was facilitated using Python libraries like Matplotlib or Seaborn, providing insightful plots and graphical representations. These visualizations helped in better understanding the patterns and variations in moisture flux convergence across the studied region in West Africa.

3.2.2 Correlation between Rainfall and Moisture Flux Convergence

The MFC averaged for West Africa from the period of 1980 to 2020 was analyzed using regression analysis in this study. The correlation between rainfall and moisture convergence was computed by:

$$r = \frac{n\sum_{i=1}^{n} X_i Y_i - \sum_{i=1}^{n} X_i \sum_{i=1}^{n} Y_i}{\sqrt{n\sum_{i=1}^{n} X_i^2 - (\sum_{i=1}^{n} X_i)^2}\sqrt{n\sum_{i=1}^{n} Y_i^2 - (\sum_{i=1}^{n} Y_i)^2}}$$

where n is the number of months, and i is the month indices; X_i is the rainfall average for West Africa; Y_i is the moisture flux convergence averaged for West Africa. Hanke et al. (2001) proposed the formula for the correlation coefficient r in the preceding equation. The Pearson correlation was used at a 95% significance level.

3.2.3 The characteristic impact of the variations in MFC on the rainfall variability

The characteristic impact (Δ) of the variations in moisture flux convergence (MFC) on the rainfall variability over West Africa was estimated from the seasonal monthly anomalies of both variables using the equation,

$$\Delta = \frac{\partial(R)}{\partial(MFC)} \times \sigma(MFC)$$

where the first term is the MFC's regression coefficient on R, the second term is the MFC's standard deviation (SD), and the last item, (mm month^{-1}), includes impacts from the domain's combined

moisture flow and rainfall efficiency that are unaffected by changing mean states (Dyn et al., 2015).

3.2.4 Rainfall Anomaly Index and Moisture Flux Convergence Anomaly Index

The anomaly index was utilized as a measurement to determine the deviation of model predictions from observed values relative to the mean of the observed values. The Anomaly Index (RAI) was considered a measure of the deviation of model predictions from observed values relative to the mean of the observed values. Insight was provided into whether the model consistently predicted values that were above or below the mean of the observed data. The RAI for a dataset y with n observations and model predictions could be calculated using the following formula:

For positive anomalies

$$RAI = 3\left[\frac{W - \bar{W}}{\bar{X} - \bar{W}}\right]$$

For negative anomalies.

$$RAI = -3\left[\frac{W - \bar{W}}{\bar{Y} - \bar{W}}\right]$$

W = recent yearly average in reference to the year RAI will be generated.

$\bar{W}$= yearly rainfall averages in millimeters;

$\bar{X}$ = 10 of the highest yearly averages in millimeters

$\bar{Y}$= 10 of the lowest yearly averages.

In this study, the RAI is adapted to compute the moisture flux convergence anomaly index to compare the two indices statistically. The two indices are then plotted together for visualization.

Table 3.1 A Classification of the Intensity of the Rainfall Anomaly Index

	Range of the RAI	Categories
RAI	Above 3	Extremely wet
	2 to 3	Very wet
	0 to 2	Wet
	-2 to 0	Dry
	-3 o -2	Very dry
	Below -3	Extremely dry

Source: Freitas (2005) adapted by Araújo et al. (2009)

3.2.5 Comparing Datasets (Error Analysis)

3.2.5.1 Root Mean Square Error (RMSE)

The root means square error is a measurement used to determine the level of absolute anticipated uncertainty between the model and the reference state (RMSE). The Root Mean Square Error (RMSE), also known as the root mean square deviation, is a common tool used to quantify the difference between the values predicted by a model and the values observed in the environment being simulated. Other names for RMSE include the root mean square error and the root mean square deviation (RMSD). These distinct discrepancies, sometimes referred to as residuals, are combined using the Root Mean Square Error to provide a single metric of predictive power. The

RMSE for a data set y with n observations and model predictions that can be calculated using the following formula:

$$RMSE = \sqrt{\frac{\sum_{i=1}^{n}\left(X_{obs,i} - X_{model,i}\right)^2}{n}}$$

Where, $X_{obs,i}$ is the observation value and $X_{model,i}$ is the forecast value.

The RMSE provides a measure of how well the model's predictions correspond to the actual observed values. Smaller RMSE values indicate that the model's predictions are closer to the observed values, while larger RMSE values indicate greater discrepancies between the model and observed data.

3.2.5.2 Mean Bias Error (MBE)

The mean bias error was used as a measurement to determine the average discrepancy between model predictions and observed values. The Mean Bias Error (MBE) was considered a measure of the average error or bias in model predictions when compared to observed values. Insight was provided into whether the model was consistently overestimated or underestimated with respect to the observed data. The MBE for a dataset y with n observations and model predictions could be calculated using the following formula:

$$MBE = \frac{1}{n}\sum_{i=1}^{n}(P_i - O_i)$$

The MBE can be positive or negative, indicating whether the model tends to overestimate or underestimate the observed values. A positive MBE suggests that the model predictions are, on average, higher than the observed values, while a negative MBE suggests that the model predictions are, on average, lower than the observed values. An MBE of zero indicates that the model predictions are, on average, unbiased.

3.2.5.3 Absolute Error (AE)

The absolute error was utilized as a measurement to determine the magnitude of the difference between model predictions and observed values without considering the direction of the error. The Absolute Error (AE) was considered a measure of the magnitude of the error between model predictions and observed values. Insight was provided into how far off the model predictions were from the observed data, regardless of whether the model overestimated or underestimated. The AE for a dataset y with n observations and model predictions could be calculated using the following formula:

$$AE = | MFC - (P - E) |,$$

The AE provides a measure of the overall magnitude of the errors, allowing for a better understanding of the model's accuracy in reproducing observed data.

3.3 Dataset

3.3.1 Observation Dataset

The density of rain gauges has a significant impact on the quality of gridded gauge datasets, which are often used as reference datasets in studies of rainfall throughout West Africa (e.g., Ama et al., 2015; Okoro et al., 2020b; Quagraine et al., 2020). Much of West Africa often has inadequate gauge coverage, and over the last several decades, gauge numbers have dramatically decreased (Quagraine et al., 2020.). Such spatiotemporal anomalies may affect the patterns and variability of represented spatial rainfall. We also utilized the Climate Hazards Group Infrared Precipitation with Stations dataset, CHIRPS (Funk et al., 2015), in addition to the gauge-only datasets. CHIRPS uses in-situ station data, CHPclim, 0.05° resolution satellite imagery, and data spanning all longitudes from 1981 to almost the present to provide gridded rainfall time-series data for trend analysis and

seasonal drought monitoring. The satellite dataset's input combines thermal infrared measurements with other data inputs, such as passive microwave retrievals and rain gauge readings, and as a result, benefits from rainfall data with high spatiotemporal resolution from a variety of sources.

After merging rain gauge data from the Global Historical Climatological Network, the Global Summary of the Day, additional private contributors, meteorological agencies, and satellite estimates, CHIRPS applies a final gauge-based bias adjustment. CHIRPS cannot be utilized as a stand-alone data source as a consequence, but it may be used to evaluate the spatial consistency of gauge-only outputs.

I used CRU-TS4.04 (CRU) as a reference dataset for the analyses that were performed for comparison with the other observations and the reanalysis datasets for the research period. To facilitate comparability, all of the study's data are regrided to a resolution of 0.50 x 0.50, which is the resolution of the observational data.

3.3.2 CORDEX Data

The Coordinated Regional Downscaling Experiment (CORDEX), which is the first worldwide effort to provide a consistent framework for downscaling experiments, was established to provide researchers with a greater opportunity to develop more reliable regional climate change scenarios. (Giorgi & Gutowski, 2015). Diverse studies have examined the performance of the RCMs participating in the CORDEX-Africa domain trials. (Okoro et al., 2020). The CORDEX models have shown the climatology and spatial variability of precipitation in WA (Akinsanola & Ogunjobi, 2017).

The simulations of CORDEX Africa comprise hindcast, historical, and prospective simulations. The ERA-Interim reanalysis drove the retrodiction runs. The RCMs were continually integrated

throughout the whole African area over 30 years, from January 1979 to December 2008, with the first year (1979) deemed spin-up time and so excluded from the study. The initial and lateral RCM borders are executed with a spatial resolution of 50 kilometers. (Gbobaniyi et al., 2014).

For the period 1960–2100, the historical and future simulations were forced by different GCMs. The simulations of the future era adhere to the RCP4.5 and RCP8.5 predictions. RCP 4.5 and RCP 8.5 were selected to reflect moderate and severe climate change scenarios, whereas all CORDEX-Africa outcomes are for the end of the 21st century (Gutowski et al., 2016)

In this work, I investigate 1981-2005 for the historical data and 2006-2100 using the RCP8.5 scenarios at a horizontal resolution of 0.44. The Earth System Grid Federation data nodes (https://esgf-index1.ceda.ac.uk/projects/esgf-ceda/) were accessed to get the monthly outputs of evaporation and precipitation, as well as specific humidity, easterly wind, and northerly wind at 850hPa (Okoro et al., 2020). This ensemble is now the most important data collection for assessing climate change on the African continent. (Soares et al., 2019). For easier comparison, all datasets were studied from 1981 to 2100 and gridded using an area-weighted average to match the resolution of the reanalysis dataset (0.5x0.5).

In this work, two RCMs were used based on their involvement in trials inside the CORDEX-Africa domain and their results for the required variables (Giorgi & Gutowski, 2015). The possible unpredictability of the reanalysis outputs may be accounted for by using several data sets. (Chen et al., 2002)

3.3.3 ERA5

The First Global Atmospheric Research Program Global Experiment, ERA-15, ERA-40, and ERA-I were precursors of the ERA-5, which is the fifth global atmospheric reanalysis product

(Hersbach et al., 2020). It is the most recent high-resolution reanalysis produced by the Integrated Forecast System (IFS Cycle 41r2) of the European Centre for Medium-Range Weather Forecast (ECMWF) to replace their ERA-Interim product. The new reanalysis is useful for climate modeling since it takes into account inputs like sea surface temperature (SST), sea ice, and aerosols. The data include 137 levels and a geographical resolution of 31 km. For its uncertainty estimations, ERA5 employs a 12-hourly 4D-Var data assimilation ensemble in addition to a 10-member ensemble of data assimilations at 63km resolution (Hersbach et al., 2020). Although there are intentions to ultimately extend the period far beyond 1950, ERA5 is now accessible from 1979 to the present. While there are several pressure levels of atmospheric data accessible, precipitation data is made up of two 2-dimensional surface level factors, namely snow, and rainfall. Precipitation is recorded as a cumulative total starting from the day's beginning. For the present research, data at 00 UTC was downloaded to estimate daily precipitation, which gives the total amount of precipitation for the previous day. This included downloading daily data from https://cds.climate.copernicus.eu with a geographic resolution of 0.25x0.25 and converting it to monthly totals and annual averages. (Arshad et al, 2021)

Table 3.2 List of CORDEX-Africa models, their description, and references.

RCM Name	Domain	Institute	Horizontal resolution	Experiment	Driving GCM	Reference
RCA4	AFR-44i	SMHI	0.44^0 x 0.44^0	RCP 4.5 Historical	MPI-M-MPI-ESM-LR	Panitz (2014)
RACMO22T	AFR-44i	KNMI	0.44^0 x 0.44^0	RCP 4.5 Historical	ICHEC-EC-EARTH	Van den Hurket al. (2014)

CHAPTER 4

RESULTS AND DISCUSSION

This chapter presents the analysis of the data and moisture flux convergence. Basic statistical analysis involving graphical tools and basic statistics such as mean bias error, absolute error, root mean square error, anomaly index, and regression analysis are performed on the dataset to ascertain the relationships between them. The results obtained from processing the data are also discussed in this chapter. Python was the software of choice used primarily in the data analysis.

4.1 Moisture Transport

The zonal and meridional moisture flux transports, qu and qv, are averaged from 1981 to 2005. In Figure 1, they are shown as arrows overlaid over the red and blue colors (MFC). The findings are consistent with Lélé & Leslie (2016) and reveal that moisture transfer occurs throughout the rainy season (May–September) from the southwest to the east of the research region from the direction of the Gulf of Guinea and the Atlantic Ocean. During the Southwest Monsoon, which is connected to the rainy season in West Africa, a southwest wind transports a strong moisture flux with moisture components from the Atlantic Ocean towards West Africa. Figure 1 shows that the moisture movement is most active in July and August. Weak moisture flows from the east to the west of the study region from March to May.

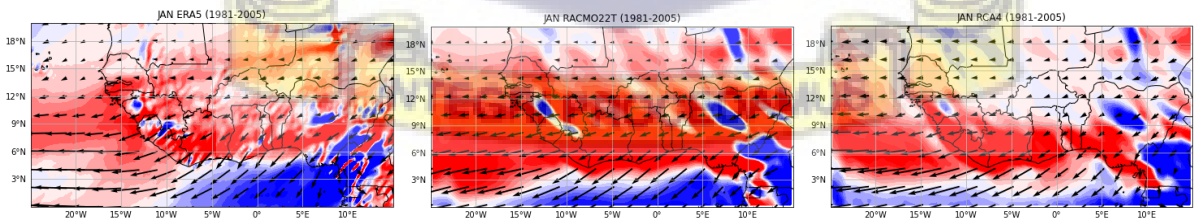

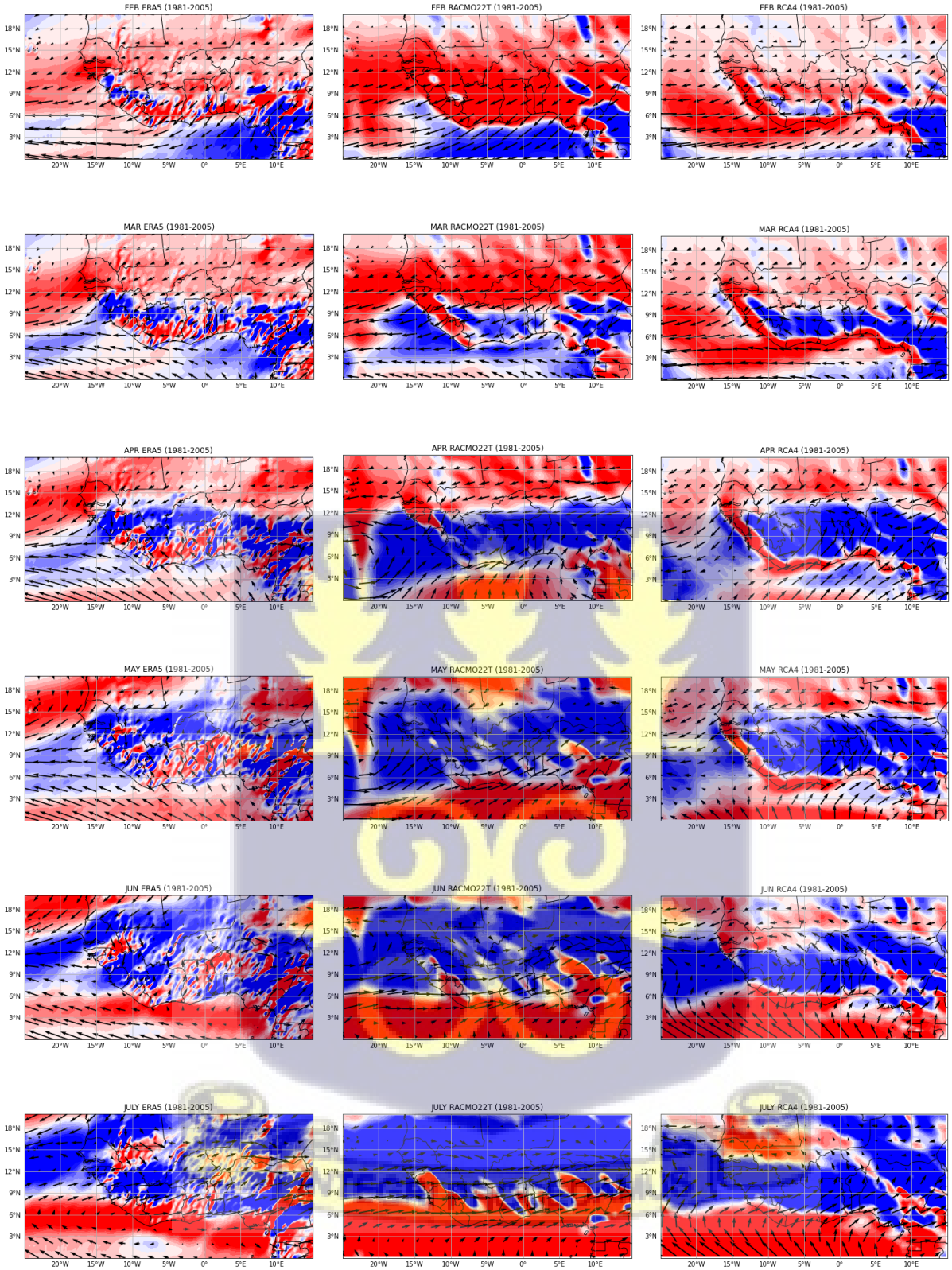

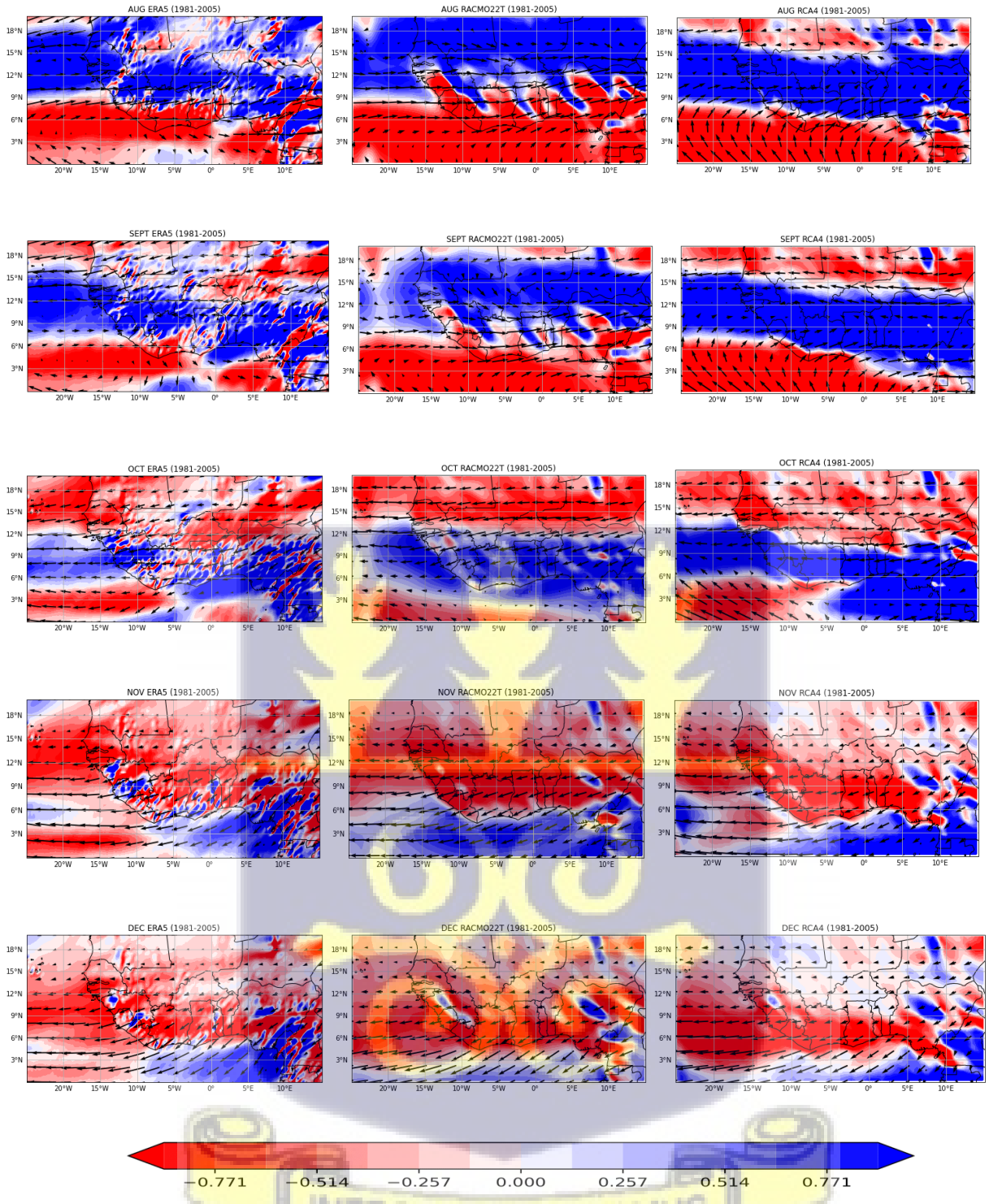

Figure 4.1 Moisture flux transport (black arrows) evolution with MFC (color shades of red and blue) from January to December (1981-2005).

4.2 Moisture Flux Convergence

The total annual moisture flux convergence in centimeters was calculated using ERA5 data from January 1981 to December 2005 and CORDEX data from January 1981 to December 2005 for the historical data. Blue represents positive MFC, whereas red represents negative MFC, which is also called VIMD. The VIMD is the polar opposite of the MFC. The rainy season begins in March and terminates in September. During the rainy season, the positive MFC (blue) covers almost the entire domain. The southern and western part, along the Guinea coast of West Africa, has higher MFC than the other parts. MFC in August is higher than in June and September. The direct transport of moisture from the Gulf of Guinea by the southwestern winds creates significant moisture convergence over West Africa, thus resulting in higher rainfall. In April, which marks the onset of the rainy season, moisture convergence is significant across West Africa. From October to December, there is a significant divergence over the North Eastern and North Western parts of the region.

Unlike the WAM, the northeast trade winds that blow over West Africa from the northeastern part to the southwestern part from November to February are dry. Because of the dryness of the Northeast Trade winds, there is an increase in the rate of evaporation during the dry season (NDJF). For this reason, a large amount of moisture departs from the domain from November to January, but input is also low. The moisture flux convergence reduces as temperature lowers in the latter part of November, and it increases with precipitation in the domain from May to September. The findings, from Figure 2, buttress the point that the quantity of moisture flux convergence decreases from January until March due to the dryness of the air entering the domain before April. The direction of the northeast trade winds can be confirmed in Figure 2.

Using the monthly average, the highest values of moisture flux convergence of over 24.3 cm y-1 were achieved using CORDEX data during the wet years 1999-2000, 1994–95, and 2003–2004, while the lowest value (11.8 cm y-1) was found during the dry year 1982-83. Equivalent results using the ERA-5 reanalysis dataset were 23.6 cm y-1 in the wet year 1999-2000 and 11.2 cm y-1 in the dry year 1982-1983, with a 24-year average of 17.2 cm y-1. Using the CORDEX dataset, average moisture flux convergence values of 16.9 cm y-1 and 19.4 cm y-1 were derived for RCA4 and RACMO22T, respectively.

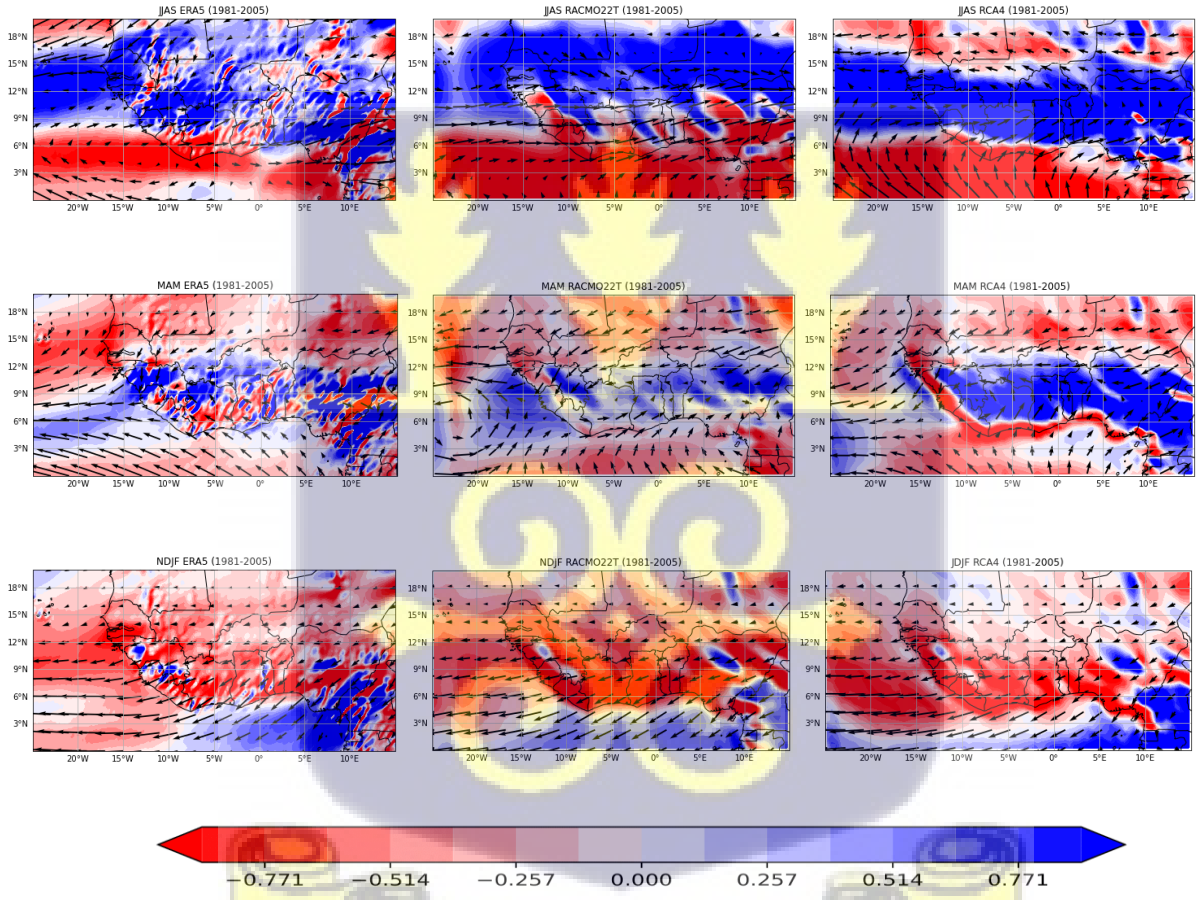

Figure 4.2 Comparisons of MFC between seasonal means, JJAS, MAM, NDJF for ERA5, RACMO22T, and RCA4 from 1981 to 2005.

4.3 Comparing rainfall distribution for RCA4, RACMO22T and CRU4.04

In comparing the rainfall distribution in West Africa among two climate models (RACMO22T and RCA4) and observational data (CRU4.04), a notable trend emerges. RCA4 consistently overestimates the rainfall in the region to a greater extent than RACMO22T. Despite this, both models exhibit a striking similarity with the observational data, CRU4.04. This suggests that while RCA4 tends to overstate precipitation levels, the underlying patterns and spatial distribution of rainfall are accurately captured by both models. The alignment of the models with observational data, especially in the context of West Africa's rainfall, underscores their ability to represent essential climatic features, highlighting the importance of considering not only the overall estimates but also the regional patterns in evaluating model performance and enhancing our understanding of West African climate dynamics.

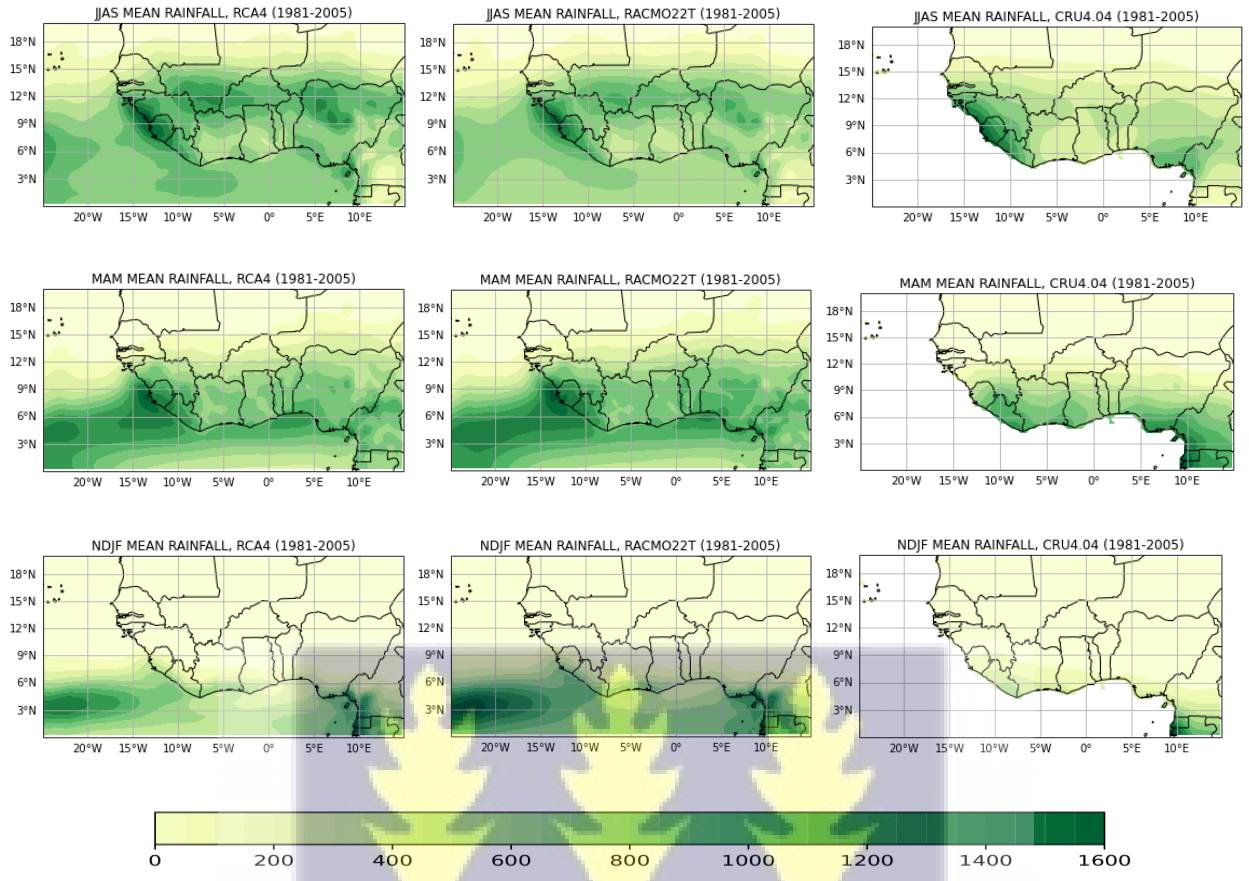

Figure 4.3 The JJAS, MAM, and NDJF, mean rainfall distribution for CRU4.04, RCA4, and RACMO22T from 1981 to 2005.

4.4 Rainfall and MFC (Rainfall Anomaly Index)

The considerable levels of anomalies in West Africa's rainfall between 1981 and 2020 may be split into two distinct phases: a wet year and a dry year. Anomalies in precipitation are positive in wet years and negative in dry years. Figure 4 provides a visualization of this.

In 1983, 1995, and 1999, the most extreme precipitation anomalies occurred with the highest positive value obtained in 1999 and the lowest negative value obtained in 1983. However, precipitation in the region has increased steadily since 1990, with a positive anomaly rate. There were 23 years of positive RAI, which had different values ranging from extremely wet to humid,

and 15 years with negative RAI, with values ranging from very dry to dry. There were more wet years than dry years. Comparing the RAI for CHIRPS and CRU in Figure 5 shows a good agreement with a correlation coefficient of 0.936. This shows that there is a very small disparity between the datasets, and as such, CHIRPS can be used instead of CRU and would produce similar results.

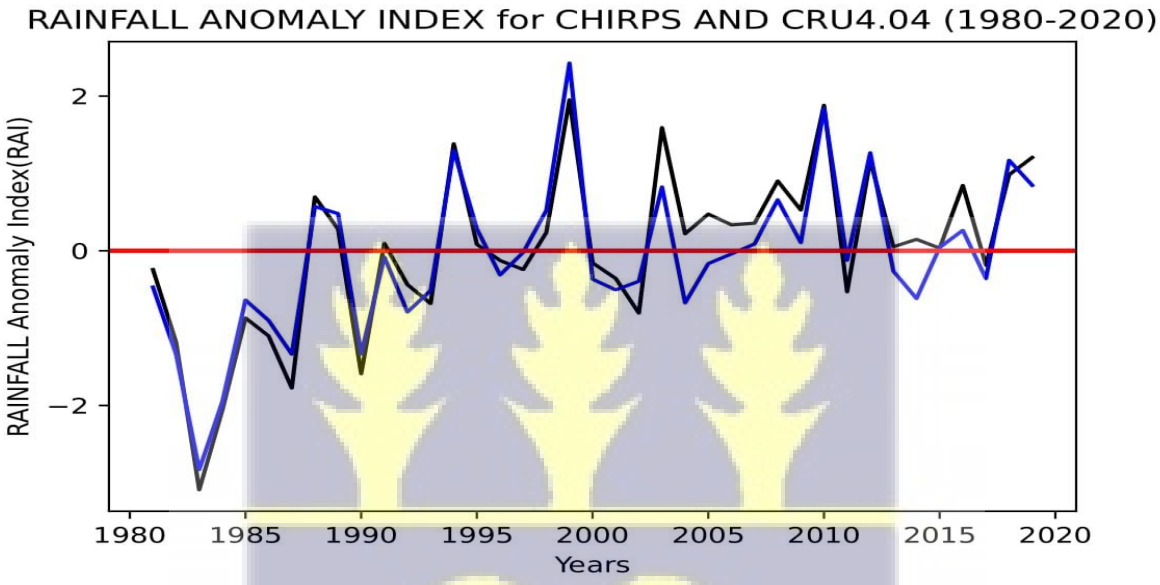

Figure 4.4 Represents the rainfall anomaly Index for climate Climate Hazards Group InfraRed Precipitation with Station data (CHIRPS)-blue line and climate research unit 4.04- black line. Showing wet years (yearly values above the red line) and dry years (yearly values below the red line) from 1980 to 2020.

4.5 Relationship between Rainfall and Moisture Convergence

The MFC over WA is high in the wet season but low amidst the dry season; rainfall is low throughout the dry season. ERA5 and CORDEX average findings for high and low MFC months demonstrate reasonably outstanding consistency (Figures 6 and 7). High MFC months have much

more precipitation and lower winds than low MFC months. This demonstrates that the effects of MFC on precipitation quantity are impacted highly by the WAM.

The influence that MFC has on precipitation is often significantly bigger than that of wind convergence, and this is one of its defining characteristics. The values obtained for the characteristic impact on precipitation were 2.53 mm/day and 1.6 mm/day, respectively, for MFC and wind convergence. The association between rainfall and MFC across WA has a strong positive correlation of 0.8315.

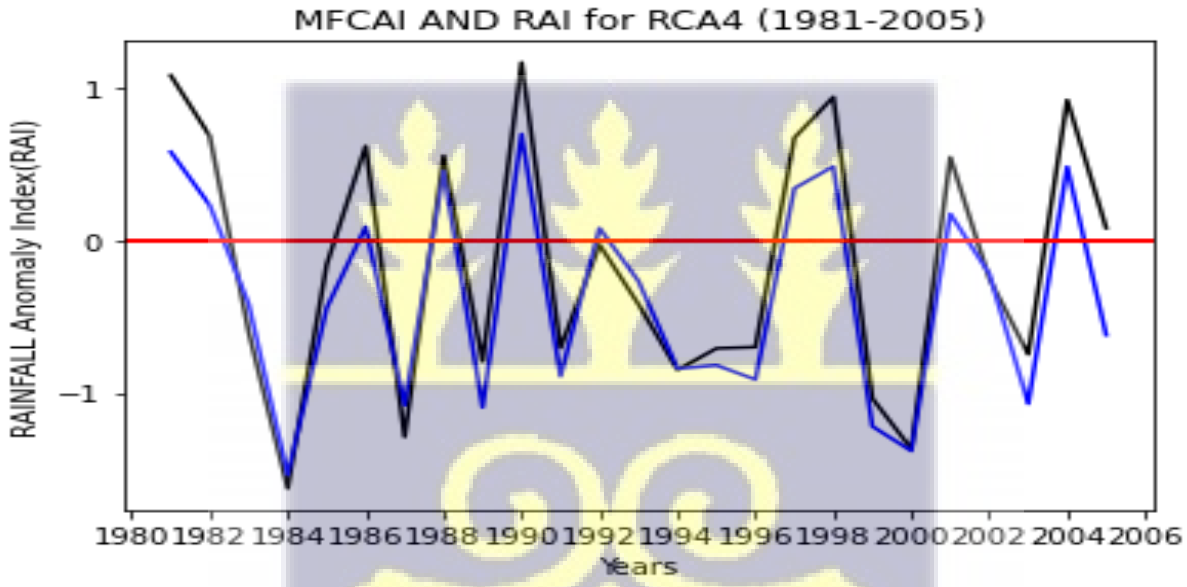

Figure 4.5 MFC anomaly index (blue line) and Rainfall anomaly index for (black line) RCA4 from 1981 to 2005.

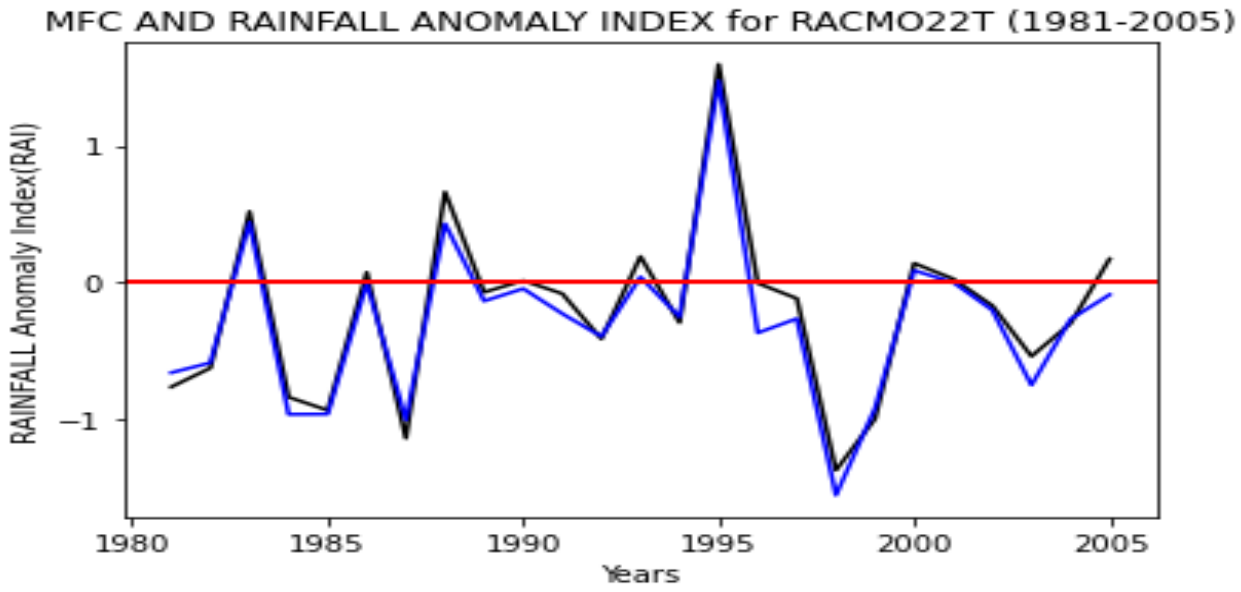

Figure 4.6 MFC anomaly index (blue line) and Rainfall anomaly index for (black line) RACMO22T from 1981 to 2005.

4.6 The Temporal Variability of Dry years and Wet years for the 21st century

New classifications for dry and wet years based on the categories of the rainfall anomaly index were presented to examine the temporal aspects of dry and wet occurrences under climate change. A year is considered to be rainy if the RAI is larger than 1. A dry year is one in which the RAI is less than -1. When the RAI is between -1 and 1, the year is considered to be normal.

To simplify the RAI analysis, the period of study was divided into three sections, namely, the early 21st century (2010-2040), the mid-21st century (2040-2070), and the end of the 21st century (2070-2100). From Fig. 11, RCA4 (RCP4.5) in the early 21st century shows six (6) wet years and eight (8) dry years. RACMO22T (RCP4.5) presents slightly different results with five (5) wet years and eleven (11) dry years. In the mid-21st century, the wet years were five (5) and the dry years were five (5) for RCA4 (RCP4.5), and RACMO22T (RCP4.5), six (6) wet years and eight (8) dry years were recorded. Three (3) wet years and seven (7) dry years were recorded for RAC4

(RCP4.5), and six (6) wet years and nine (9) dry years were recorded for RACM22T. There were more dry years than wet years from both RCMs. It was determined that the occurrence rate of drought decreased in the mid-21st century and increased again towards the end of the century. This implies that the region is likely to be drier towards the end of the century.

The RCP 8.5 shows a different result with the same number of wet and dry years for RCA4 at the beginning of the century slightly wetter mid-century and more drought towards the end of the century. RACMO22T showed dry early and mid-century and wet years towards the end of the century.

4.7 The Seasonal Variability of MFC for RCP4.5 and RCP8.5

From 2006 to 2100, the RCP 4.5 and RCP 8.5 models were used to explore the monthly averages, JJAS mean, MAM mean, and NDJF mean. The models demonstrate that the 850 hPa atmospheric moisture flux transfer over land the Gulf of Guinea and the northern tropical Atlantic has parallels for the RCP 4.5 scenario. There are also parallels in the patterns of the MFC that can be seen in every climatological indicator.

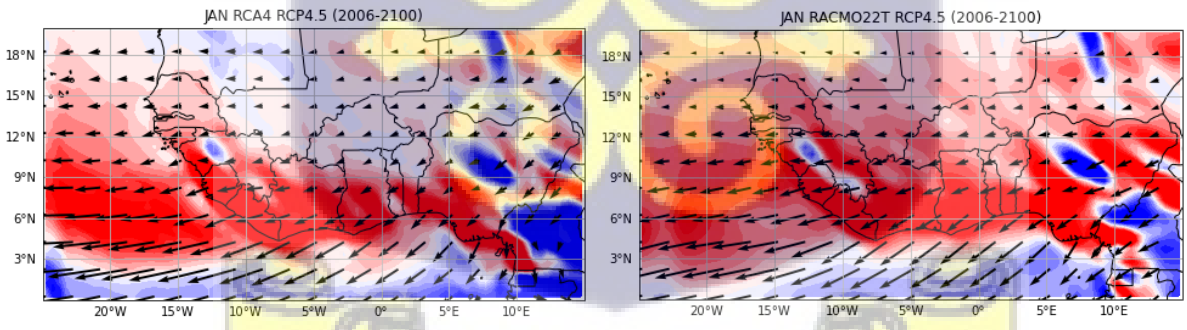

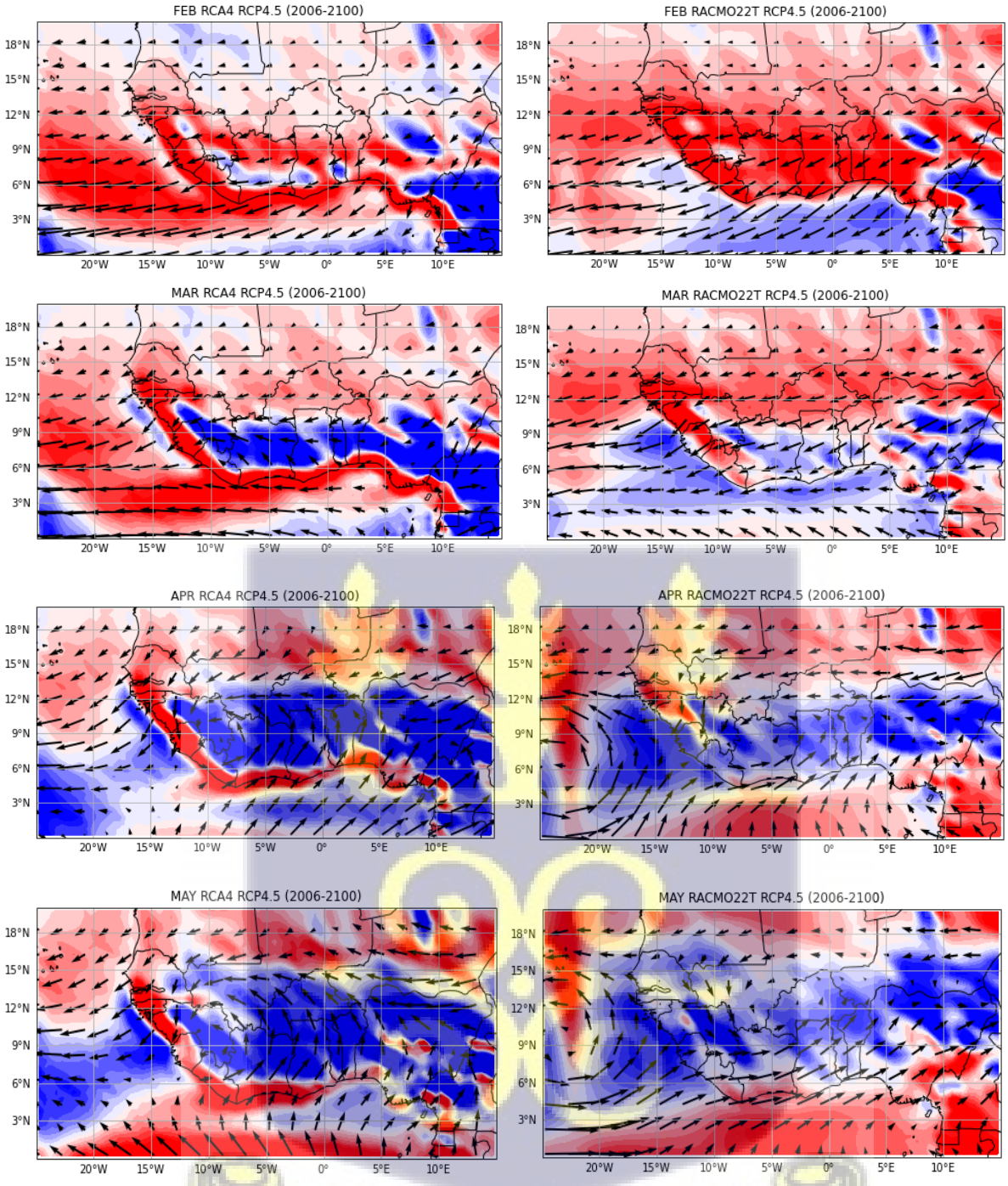

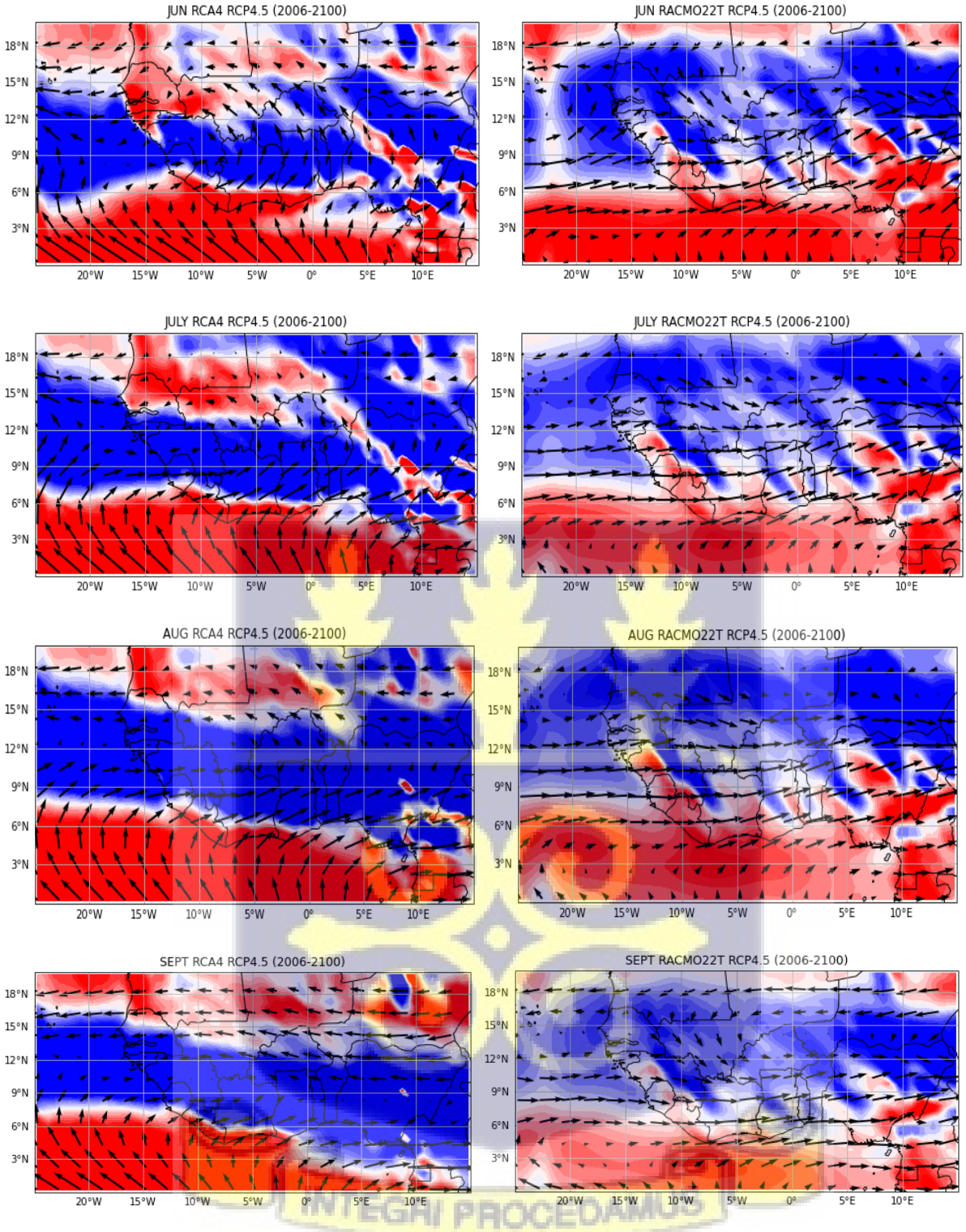

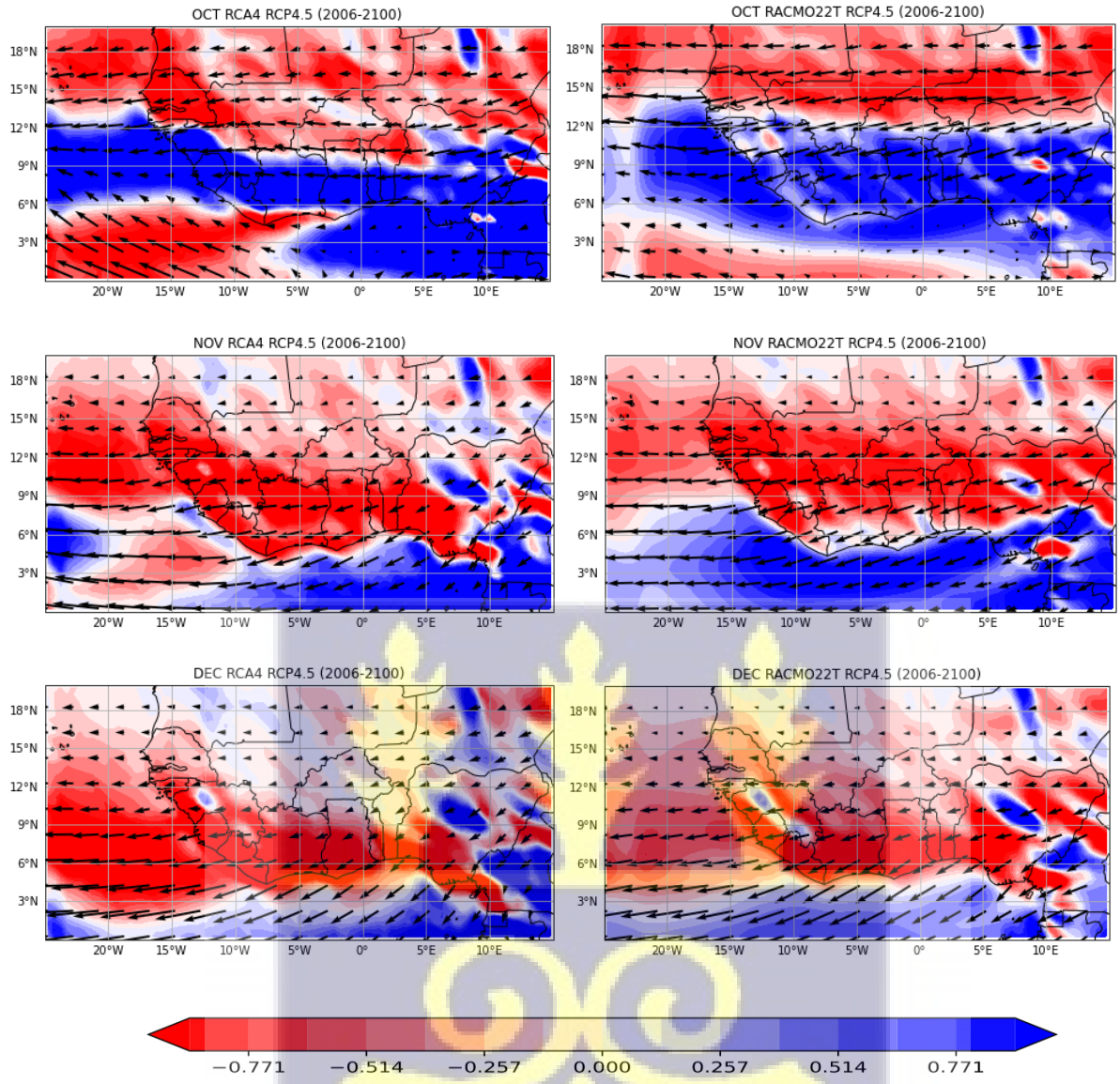

Figure 4.7 MFC (color shades) and moisture transport (black arrows) for RCA4 and RACMO22T (RCP 4.5) from 2006 to 2100.

Additionally, the RCP 8.5 experiment demonstrates that the 850 hPa atmospheric moisture flux transfer across land, the Gulf of Guinea, and the northern tropical Atlantic all have several commonalities (Figure 7). The MFC patterns are likewise comparable, even though their intensities differ. Again, the highest values were predicted to be in the Gulf of Guinea and along the shores of Guinea and Sierra Leone when they were simulated.

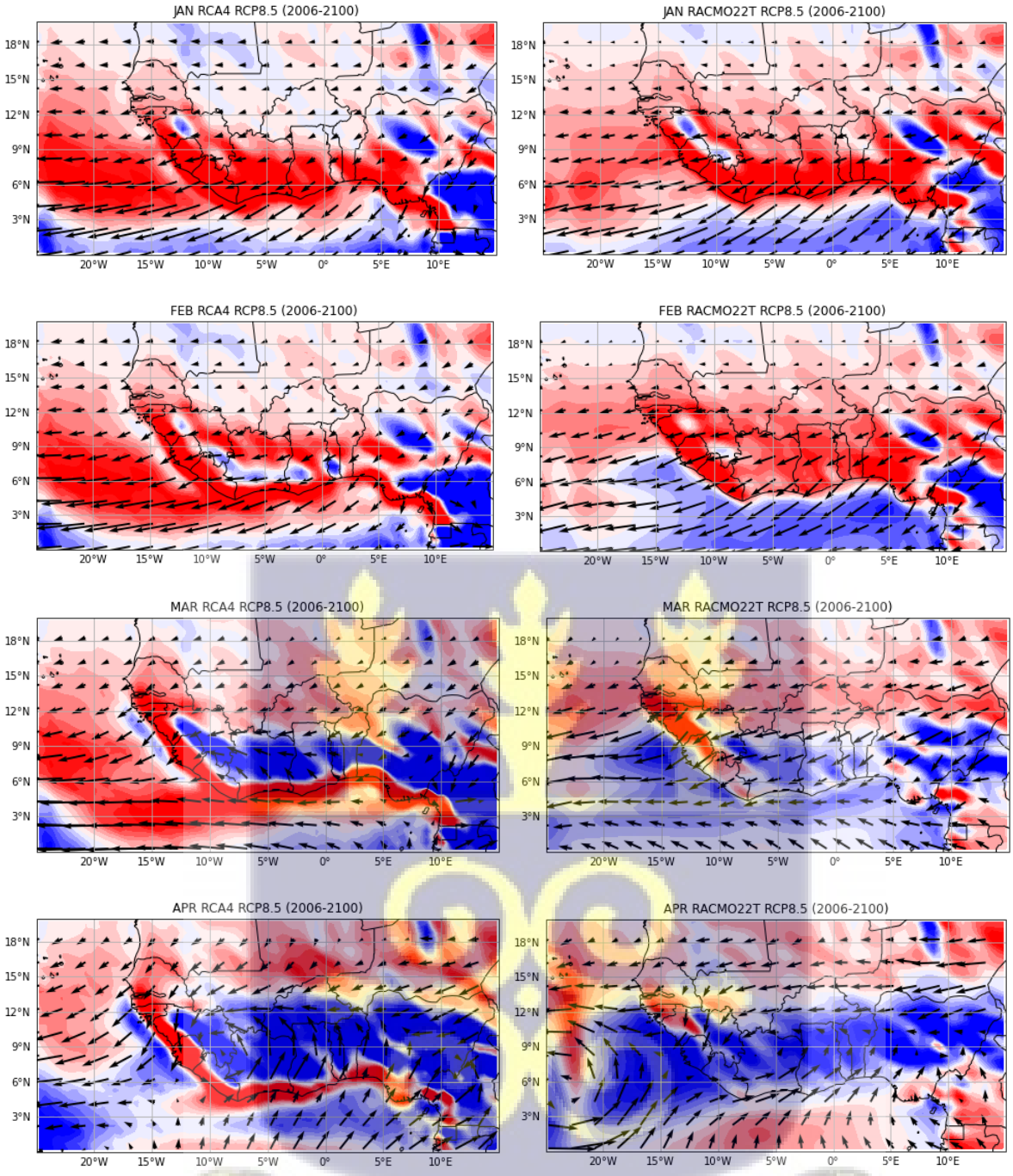

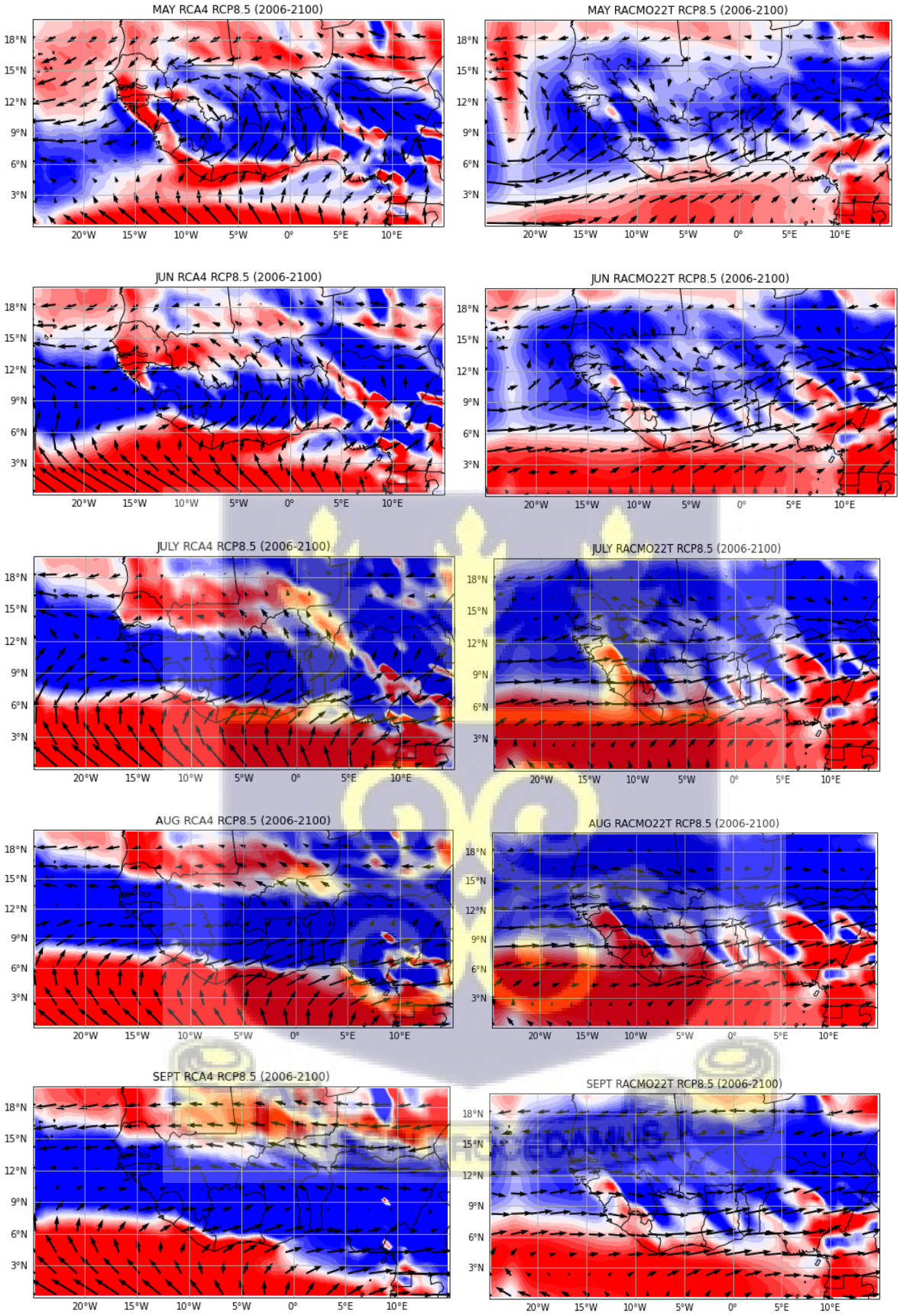

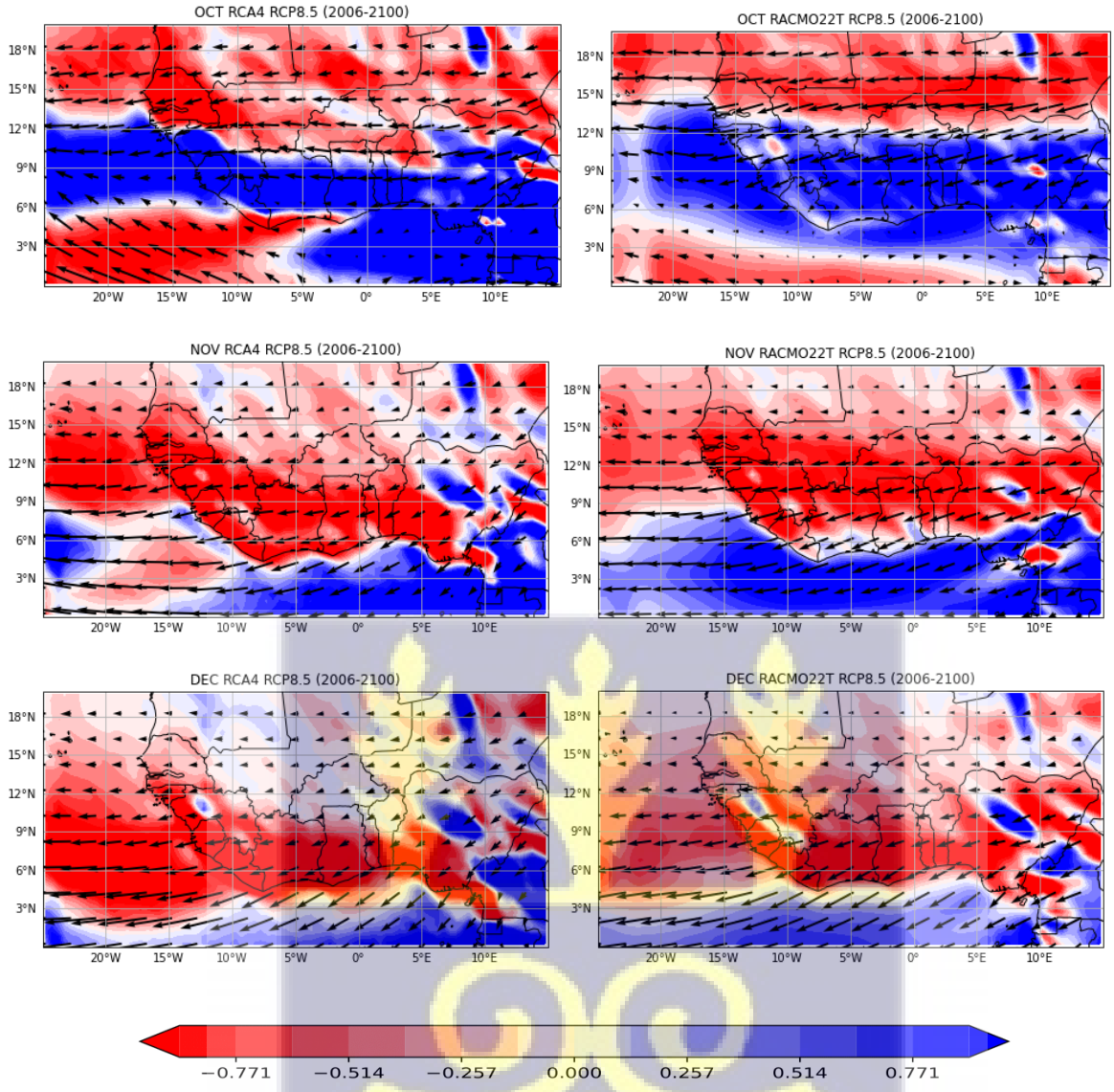

Figure 4.8 MFC (color shades) and moisture transport (black arrows) for RCA4 and RACMO22T (RCP 8.5) from 2006 to 2100.

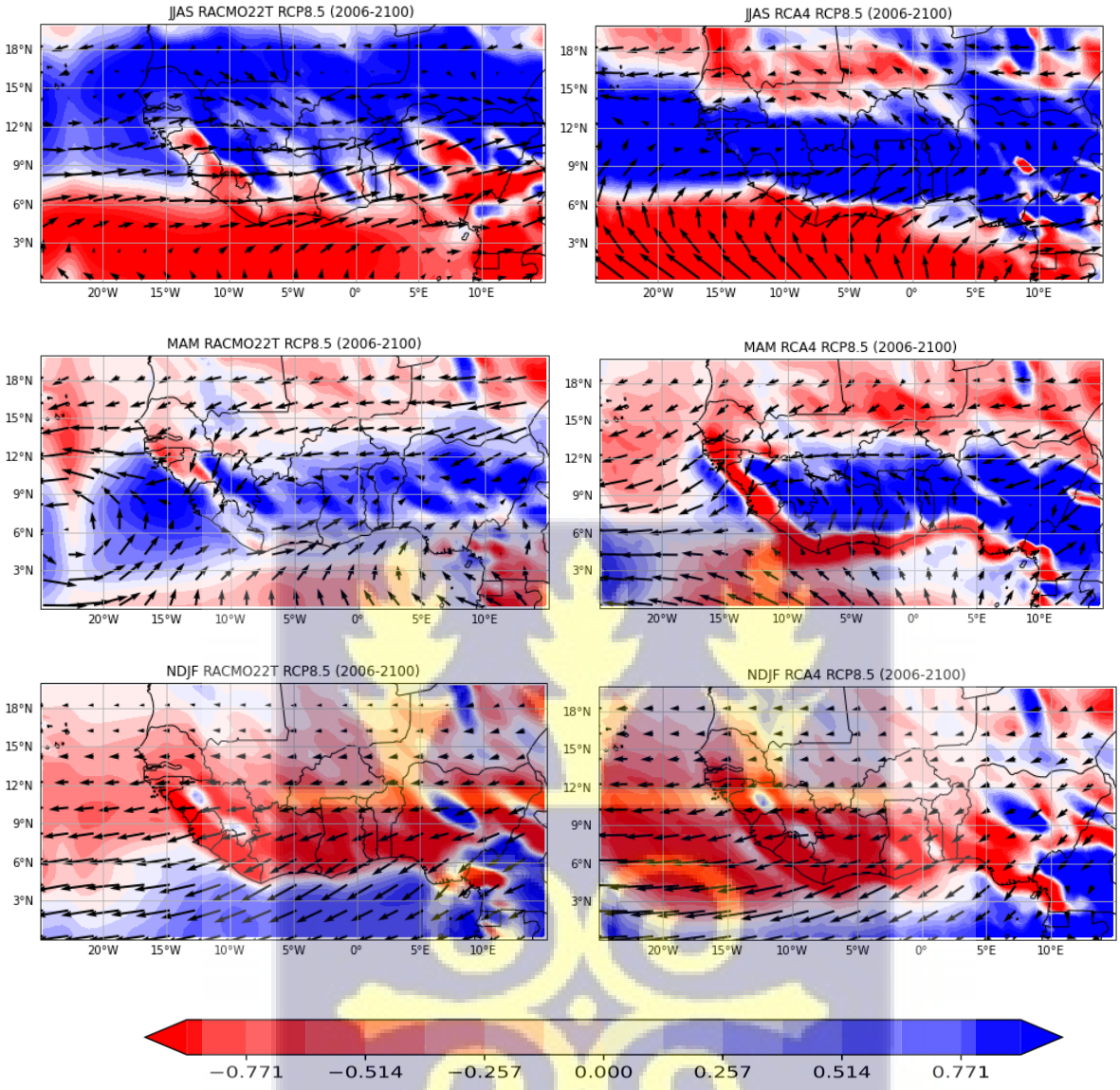

Figure 4.9 Seasonal means of MFC (color shades) and moisture transport (black arrows) for RCA4 and RACMO22T (RCP 8.5) from 2006 to 2100.

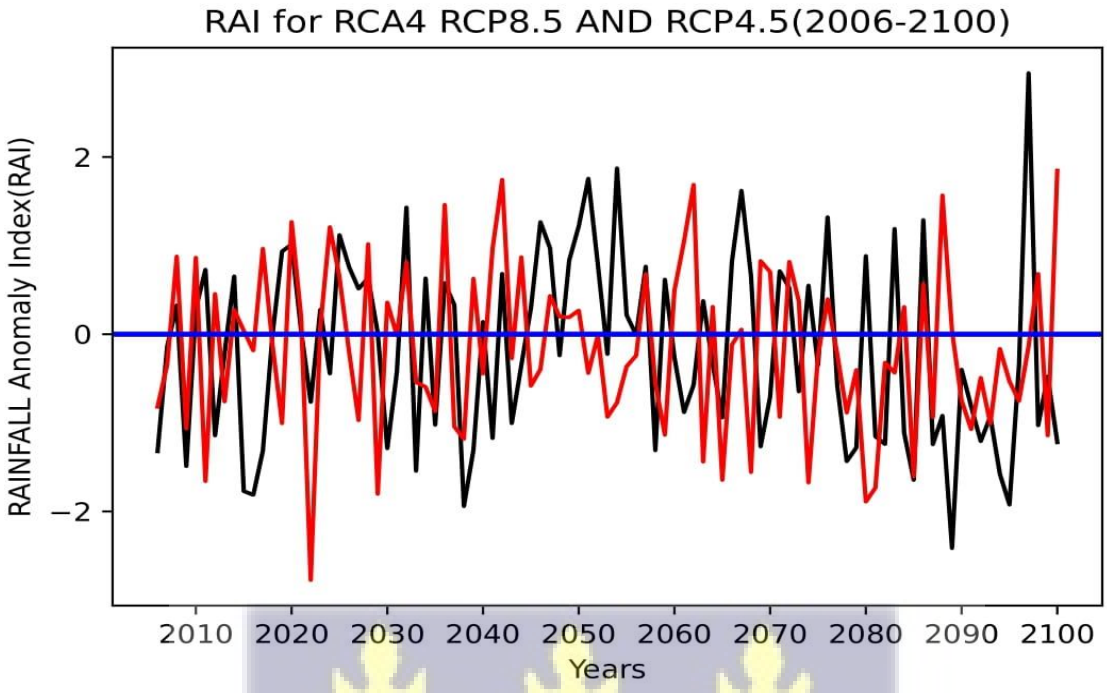

Figure 4.10 Rainfall Anomaly Index for RCA4 rcp8.5(black line) and rcp4.5(red line)

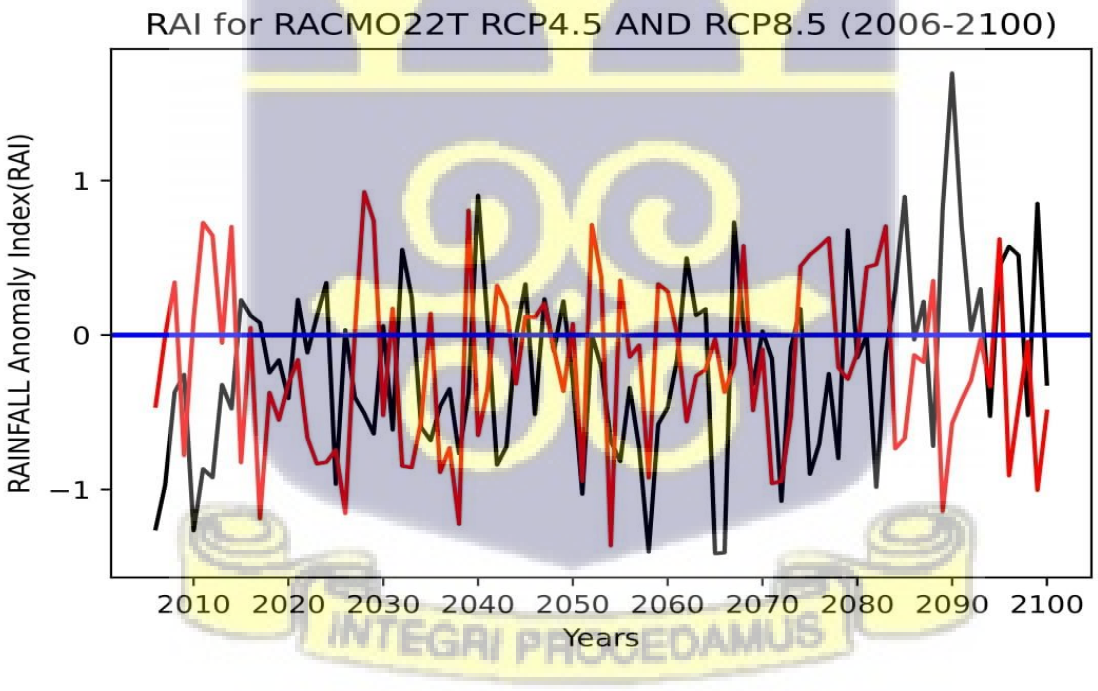

Figure 4.11 Rainfall Anomaly Index for RACMO22T rcp8.5(black line) and rcp4.5(red line)

The evaluation research used absolute error to determine the absolute value of the difference between the calculated and real values. It might be argued that P - E can be approximated using MFC if the absolute error is relatively modest. Table 1 in this research displays the absolute error of P-E and MFC. The fact that P - E and MFC have such a modest difference suggests that MFC may be used to estimate P - E. The number that represents the volume of water in the atmosphere is known as the P-E value.

Table 4.1 Absolute error values between computed MFC and E-P values.

Month	Absolute Error	Month	Absolute Error
January	0.000023	July	0.000012
February	0.000029	August	0.000017
March	0.000088	September	0.000064
April	0.000057	October	0.000056
May	0.000077	November	0.000021
June	0.000049	December	0.000032

Table 4.2 Results obtained for comparing the CORDEX data to ERA5 statistically. r is the coefficient of regression; MBE represents the Mean bias error and RMSE is the root mean square error.

	Model	r	MBE	RMSE
MFC	RCA4	0.59	-0.0964	0.486
	RACMO22T	0.43	-0.0682	0.395

CHAPTER 5

CONCLUSION AND RECOMMENDATION

5.1 Conclusion

Understanding the variability of moisture flux and moisture flux convergence is essential for comprehending the variability of West African Monsoon (WAM) precipitation and its potential variations in response to climate change scenarios. The intricate interplay between atmospheric moisture transport and convergence critically influences the distribution and intensity of rainfall in this region.

It can be concluded from this research that during the rainy season (May to September), a dynamic movement of moisture transfer occurs from the southwest to the east of the study region, originating from the direction of the Gulf of Guinea and the Atlantic Ocean. This moisture-laden airflow significantly contributes to the WAM, fueling the intense rainy season that characterizes West Africa. Understanding the seasonal behavior of this moisture transfer is crucial for predicting and preparing for the impacts of these seasonal shifts on various sectors such as agriculture and water resource management.

During the WAM season, which is intricately connected to the rainy season in West Africa, a prevailing southwest wind propels a strong moisture flux carrying vital moisture components from the Atlantic Ocean toward the region. In July and August, the movement of this moisture reaches its peak, marking a critical period for agricultural planning and ecological processes.

ERA5 and CORDEX data, renowned for their reliability and accuracy, were utilized to compute the total yearly moisture flux convergence in centimeters. The findings revealed that moisture flux convergence tends to be higher in the southern and western portions of West Africa, particularly around the Guinea coast. This information is fundamental for understanding regional variations in precipitation and planning for potential shifts in these patterns in response to changing climate dynamics.

Moreover, the study investigated the stability of ERA5 and CORDEX data, demonstrating that high moisture flux convergence months are associated with substantially more precipitation and lower wind speeds compared to low moisture flux convergence months. This emphasizes the significant influence of the West African Monsoon (WAM) on the impacts of moisture flux convergence on precipitation amounts, underscoring the complexity of regional climate systems.

Rainfall and moisture flux convergence exhibit a strong positive correlation of 0.8323 over West Africa, highlighting the direct relationship between these factors and further validating the importance of moisture flux convergence as a determinant of rainfall patterns in the region.

Looking ahead to the future, projections from 2006 to 2100 using the RCP 4.5 and RCP 8.5 models indicate an alarming trend. Both scenarios forecast more dry years than wet years, indicating a trajectory toward increased aridity and drier climatic conditions in the latter half of the century. The 850 hPa atmospheric moisture flux transfer across the land, the Gulf of Guinea, and the northern tropical Atlantic exhibit parallels in both the RCP 4.5 and RCP 8.5 experiments. These projections highlight the urgent need for robust climate adaptation and mitigation strategies to mitigate the potential adverse effects of climate change on the West African region.

Understanding the dynamics of moisture flux and moisture flux convergence in West Africa is of utmost importance for climate modeling, water resource management, and formulating sustainable strategies for a region highly dependent on agricultural activities and vulnerable to climate change impacts. Further research and proactive measures are imperative to ensure the resilience and sustainability of West Africa's ecosystems and communities in the face of evolving climate patterns.

5.2 Recommendations

The knowledge gained from this investigation will be used to better understand how atmospheric moisture and large-scale circulations affect precipitation in the future. Future research should expand on the findings of this study to fully understand the effects of the dynamics of moisture flux convergence on a global scale.

An integrated approach that involves collaboration between meteorologists, climate scientists, policymakers, and stakeholders should be established. A comprehensive climate modeling framework that incorporates the insights gained from this research should be developed. This should guide policy formulation to address the potential impacts of changing moisture flux patterns on West African rainfall and climate.

The expansion and enhancement of meteorological monitoring networks and data collection systems across West Africa should be invested in. Robust data on moisture flux, atmospheric dynamics, and precipitation are fundamental for accurate climate modeling and prediction, which in turn will aid in the development of effective strategies to mitigate climate-related risks.

Sustainable water resource management strategies that consider the influence of moisture flux convergence on regional precipitation should be developed. Efficient water usage practices, conservation efforts, and the integration of renewable energy sources should be encouraged to mitigate potential water scarcity challenges arising from changing rainfall patterns.

Collaboration and knowledge sharing at an international level to address climate resilience in West Africa should be fostered. Collaboration with neighboring countries and global organizations to develop a unified approach towards climate adaptation and mitigation should be undertaken. Sharing best practices and pooling resources can significantly enhance the region's ability to combat the challenges posed by changing moisture flux patterns.

References:

Banacos, P. C., & Schultz, D. M. (2005). The use of moisture flux convergence in forecasting convective initiation: Historical and operational perspectives. *Weather and Forecasting*, *20*(3), 351–366. https://doi.org/10.1175/WAF858.1

Bielli, S., & Roca, R. (2010). Scale decomposition of atmospheric water budget over West Africa during the monsoon 2006 from NCEP/GFS analyses. *Climate Dynamics*, *35*(1), 143–157. https://doi.org/10.1007/s00382-009-0597-5

Cadet, D. L., & Nnoli, N. O. (1987). Water Vapour Transport Over Africa and the Atlantic Ocean During Summer 1979. *Quarterly Journal of the Royal Meteorological Society*, *113*(476), 581–602. https://doi.org/10.1002/qj.49711347609

Chen, R., & Tomassini, L. (2015). The Role of Moisture in Summertime Low-Level Jet Formation and Associated Rainfall over the East Asian Monsoon Region. *Dynamics, Geophysical Fluid Physics, Atmospheric*, 3871–3890. https://doi.org/10.1175/JAS-D-15-0064.1

Dyn, C., Lélé, M. I., & Leslie, L. M. (2016). Intraseasonal variability of low-level moisture transport over West Africa. *Climate Dynamics*. https://doi.org/10.1007/s00382-016-3334-x

Dyn, C., Wei, J., Su, H., & Liang, Z. (2015). Impact of moisture flux convergence and soil moisture on precipitation : a case study for the southern United States with implications for the globe. *Climate Dynamics*. https://doi.org/10.1007/s00382-015-2593-2

Egbebiyi, T. S., Lennard, C., Crespo, O., Mukwenha, P., Lawal, S., & Quagraine, K. (2019). Assessing future spatio-temporal changes in crop suitability and planting season over West Africa: Using the concept of crop-climate departure. *Climate*, *7*(9). https://doi.org/10.3390/cli7090102

Gimeno, L., Dominguez, F., Nieto, R., Trigo, R., Drumond, A., Reason, C. J. C., Taschetto, A. S., Ramos, A. M., Kumar, R., & Marengo, J. (2016). Major Mechanisms of Atmospheric Moisture Transport and Their Role in Extreme Precipitation Events. *Annual Review of Environment and Resources*, *41*(1), 117–141. https://doi.org/10.1146/annurev-environ-110615-085558

Gimeno, L., Dominguez, F., Nieto, R., Trigo, R., Drumond, A., Reason, C. J. C., Taschetto, S., Ramos, A. M., & Kumar, R. (2016). *Major Mechanisms of Atmospheric Moisture Transport and their Role in Extreme Precipitation Events*. *June*, 1–25. https://doi.org/10.1146/annurev-environ-110615-085558

Gong, C., & Eltahir, E. (1996). Sources of moisture for rainfall in West Africa. *Water Resources Research*, *32*(10). https://doi.org/10.1029/96WR01940

Hanke, J. E., Wichern, D. W., & Reitsch, A. G. (2001). The Evaluation of Forecasting Methods at an Institutional Foodservice Dining Facility. *Business Forecasting (7th Ed.). NJ, USA: Prentice- Hall*, *December 2001*. https://doi.org/10.1080/10913211.2003.10653769

Klutse, N. A. B., Quagraine, K. A., Nkrumah, F., Quagraine, K. T., Berkoh-Oforiwaa, R., Dzrobi, J. F., & Sylla, M. B. (2021). The Climatic Analysis of Summer Monsoon Extreme Precipitation Events over West Africa in CMIP6 Simulations. *Earth Systems and Environment*, *5*(1), 25–41. https://doi.org/10.1007/s41748-021-00203-y

Lélé, M. I., Leslie, L. M., & Lamb, P. J. (2015). Analysis of low-level atmospheric moisture transport associated with the West African monsoon. *Journal of Climate*, *28*(11), 4414–4430. https://doi.org/10.1175/JCLI-D-14-00746.1

Ndehedehe, C. E., Ferreira, V. G., & Agutu, N. O. (2019). Hydrological controls on surface vegetation dynamics over West and Central Africa. *Ecological Indicators*, *103*. https://doi.org/10.1016/j.ecolind.2019.04.032

Okoro, U. K., Chen, W., Nath, D., & Nnamchi, H. C. (2020). Variability and trends of atmospheric moisture in recent West African monsoon season and the Coordinated Regional Downscaling Experiment-Africa projected 21st-century scenarios. *International Journal of Climatology*, *40*(2), 1149–1163. https://doi.org/10.1002/joc.6261

Population Division |. (n.d.). Retrieved July 25, 2022, from https://www.un.org/development/desa/pd/

Quagraine, K. A., Nkrumah, F., Klein, C., Ama, N., Klutse, B., & Quagraine, K. T. (2020). West African Summer Monsoon Precipitation Variability as Represented by Reanalysis Datasets. *Climate MDPI*, *1*, 1–18.

Sultan, B., & Janicot, S. (2003). The West African monsoon dynamics. Part II: The "preonset" and "onset" of the summer monsoon. *Journal of Climate*, *16*(21). https://doi.org/10.1175/1520-0442(2003)016<3407:TWAMDP>2.0.CO;2

Sylla, M. B., Diallo, I., & Pal, J. S. (2013). West African Monsoon in State-of-the-Science Regional Climate Models. *Climate Variability - Regional and Thematic Patterns*. https://doi.org/10.5772/55140

van Zomeren, J., & van Delden, A. (2007). Vertically integrated moisture flux convergence as a predictor of thunderstorms. *Atmospheric Research*, *83*(2-4 SPEC. ISS.), 435–445. https://doi.org/10.1016/j.atmosres.2005.08.015

Wang, K. yan, Li, Q. fang, Yang, Y., Zeng, M., Li, P. cheng, & Zhang, J. xiang. (2015). Analysis of spatio-temporal evolution of droughts in Luanhe River Basin using different drought indices. *Water Science and Engineering*, *8*(4), 282–290. https://doi.org/10.1016/j.wse.2015.11.004